

INSTITUTO TECNOLÓGICO DE COSTA RICA
BIOLOGY FACULTY

“ESTABLISHMENT AND CHARACTERIZATION OF A BRAIN CELL CULTURE
MODEL SYSTEM OF MYOTONIC DYSTROPHY TYPE 1”

REPORT FOR THE FINAL GRADUATION PROJECT TO OBTAIN THE TITLE OF
BACHELOR DEGREE

Annette Vaglio Garro

CARTAGO, AGOSTO 2011.



INSTITUTO TECNOLOGICO DE COSTA RICA
BIOLOGY FACULTY

REPORT FOR THE FINAL GRADUATION WORK

TITLE:
ESTABLISHMENT AND CHARACTERIZATION OF A BRAIN CELL CULTURE
MODEL SYSTEM OF MYOTONIC DYSTROPHY TYPE 1

Annette Vaglio Garro



CARTAGO, 2011.

ESTABLISHMENT AND CHARACTERIZATION OF A BRAIN CELL CULTURE MODEL SYSTEM OF MYOTONIC DYSTROPHY TYPE 1

Annette Vaglio Garro*

ABSTRACT

Myotonic dystrophy type 1 (DM1) is an autosomal dominant genetic disease caused by the expansion of an unstable CTG repeat in the 3'UTR of the dystrophin myotonia-protein kinase (DMPK) gene. DM1 is the most common form of adult muscular dystrophy. It was initially considered as a muscle disease, but today it is known that DM1 is a multisystemic disease that affects many tissues and organs, including the central nervous system (CNS). Indeed, DM1 patients present debilitating neurological manifestations, such as hypersomnia, cognitive and learning impairment. Congenital DM1 shows severe mental retardation. The unsteady CTG sequence in DM1 tends to expand in size when it is transmitted vertically from one generation to the next. Intergenerational trinucleotide repeat instability serves as the molecular explanation of the phenomenon of anticipation, meaning the increasing severity and decreasing age of onset in successive generations of a DM1 families. The repeat is also unstable in somatic tissues, continuing to expand throughout the patient's life.

Important symptoms of DM1 are explained by the nuclear accumulation of toxic, expanded *DMPK* transcripts and subsequent deregulation of RNA-binding proteins, which leads to missplicing in multiple tissues, including brain. However the molecular pathways contributing to DM1 neuropsychological dysfunction are still unknown.

To investigate the disease pathogenesis, DMSXL transgenic mice, carrying large CTG expansions (>1000 repeats) within the human DM1 locus, were generated and studied. In the CNS, these animals show RNA missplicing, as well as Tau hyperphosphorylation, recreating, to a certain extent, the spliceopathy and tauopathy described in humans. A global proteomic approach and the study of candidate genes on DMSXL brains revealed molecular abnormalities in proteins involved in the regulation of calcium metabolism. These findings suggest that the DM1 CTG expansions may affect calcium homeostasis in the CNS.

To validate this hypothesis, neuroblastoma and astrogloma cell lines have been transfected with a large CTG repeat expansion. These cell model systems recreate important features of the DM1 molecular pathology, such as toxic RNA accumulation in the nuclei, missplicing of critical candidate genes. Nevertheless, no obvious splicing abnormalities were detected in the list of genes involved in calcium metabolism, selected for this study.

In contrast to the findings reported in skeletal muscle and heart of DM1 patients, CELF1 expression was not significantly changed by the CTG expansion in cultured brain cells.

In conclusion, the presence of foci and missplicing of some candidate genes validates our brain model system of DM1-associated RNA toxicity. However, the system may require further studies and refinement to perform functional analysis of calcium metabolism and flux at later stages.

Key words: myotonic dystrophy, calcium metabolism, transgenic mice, RNA toxicity, alternative splicing, cell culture model system.

FINAL GRADUATION REPORT. Biology Faculty, Instituto Tecnológico de Costa Rica, Cartago, Costa Rica, 2011.

ESTABLISHMENT AND CHARACTERIZATION OF A BRAIN CELL CULTURE MODEL SYSTEM OF MYOTONIC DYSTROPHY TYPE 1

Annette Vaglio Garro*

RESUMEN

La Distrofia Miotónica tipo 1 (DM1) es una enfermedad genética autosómica dominante causada por la expansión inestable de las repeticiones CTG en la región 3'UTR del gen de la distrofia miotónica de una proteína kinasa (DMPK). DM1 es la forma adulta más común de distrofia muscular. Inicialmente fue considerada como una enfermedad muscular, hoy en día se sabe que DM1 es una enfermedad multisistémica que afecta a varios tejidos y órganos, incluyendo el sistema nervioso central (SNC). En efecto, los pacientes con DM1 presentan debilitamiento neurológico, así como hipersomnolencia, discapacidades cognitivas y de aprendizaje. La forma congénita de DM1 muestra retardo mental severo. La poca estabilidad de la secuencia CTG en DM1 tiende a expandirse en tamaño cuando se transmite de manera vertical de una generación a la siguiente. El desequilibrio de las repeticiones trinucleótidas intergeneracionales sirve como explicación molecular del fenómeno de anticipación, indicando un aumento en la severidad y una disminución en la edad de inicio en generaciones sucesivas de una familia con DM1. La repetición también es inestable en tejidos somáticos, expandiéndose a través de la vida del paciente.

Algunos síntomas importantes de DM1 son explicados por la acumulación nuclear de toxinas, transcritos extendidos de DMPK y subsecuentemente la desregulación de ARNs que unen proteínas, lo cual origina el editaje incorrecto en múltiples tejidos, incluyendo el cerebro. Por otro lado el mecanismo molecular que contribuye a la neurodisfunción psicológica en DM1 sigue siendo desconocido.

Para investigar la patogénesis de la enfermedad, se creó y estudio el ratón transgénico DMSXL, que contiene largas expansiones de CTG (>1000 repeticiones) de humanos. En el SNC, estas anomalías muestran missplicing del ARN, así como la hiperfosforilación de Tau, recreando la spliceopatía y taupatía descrita en humanos. Un enfoque global proteómico y el estudio de genes candidatos en muestras de cerebro del ratón DMSXL revela anomalías moleculares en proteínas involucradas en la regulación del metabolismo del calcio. Estos descubrimientos sugieren que las expansiones de la repetición CTG en DM1 pueden afectar la homeostasis de calcio en el SNC.

Para validar esta hipótesis, líneas celulares de neuroblastoma y astroglioma fueron transfectadas con expansiones de las repeticiones de CTG. Este modelo celular recrea importantes características de la patología molecular de DM1, como la acumulación de ARN tóxico en el núcleo y el *missplicing* en genes candidatos críticos. Sin embargo, no se detectó anomalías en el proceso de corte y empalme para la lista de genes candidatos analizados y relacionados al metabolismo del calcio en este estudio.

En contraste con lo reportado en estudios previos de muestras musculares y cardíacas de pacientes con DM, los cambios en la expresión de CELF1 no fueron significativos en las células cerebrales que contenían la expansión de CTG.

En conclusión, la presencia de *foci* y *missplicing* en algunos genes candidatos valida este sistema modelo de células cerebrales como útil para estudiar la enfermedad DM1 asociado a la toxicidad del ARN. Por otro lado, el sistema requiere otros estudios y el desarrollo refinado de análisis funcionales del metabolismo y flujo de calcio en etapas posteriores.

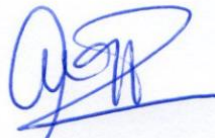
Palabras claves: distrofia miotónica, metabolismo del calcio, ratón transgénico, toxicidad del ARN, splicing alternativo, sistema modelo de cultivo celular.

REPORTE FINAL DE GRADUACION. Escuela de Biología, Instituto Tecnológico de Costa Rica, Cartago, Costa Rica, 2011.

ESTABLISHMENT AND CHARACTERIZATION OF A BRAIN CELL CULTURE
MODEL SYSTEM OF MYOTONIC DYSTROPHY TYPE 1

Report presented for the Biology Faculty as partial requirement to obtain the title of
Bachelor Degree in Biotechnology Engineering.

Court Evaluator



Dr. Mario Gomes-Pereira,
Research Associate-INSERM



Olga Rivas Solano, *MSc.*
Assessor Professor -ITCR



Carolina Centeno Cerdas, *MSc.*
Reader-ITCR

*To my family who support me
through all my education process*

ACKNOWLEDGEMENTS

I wish to record my thanks to the following organizations and individuals for their assistance during this work:

El Ministerio de Ciencia y Tecnología (MICIT) and El Consejo Nacional para Investigaciones Científicas y Tecnológicas (CONICIT) for the financial contributions that allowed me to do my internship abroad.

La Vicerrectoría de Vida Estudiantil of the Instituto Tecnológico de Costa Rica, for giving a percentage of the economic resources needed to develop my internship abroad.

All the staff of the Institut National de la Santé et de la Recherche Medicale (INSERM, Unit 781) for providing reagents, equipment, and the creative mind of the project.

To INSERM U781 laboratory. Especially to Dr. Mario Gomes-Pereira and Msc. Géraldine Sycot for their instruction and guidance during the research process.

Members of the Court Evaluator, for their valuable guidance and especially to Dr. Mario Gomes-Pereira and Dr. Genevieve Gourdon for welcoming me into their laboratory and assigning me a research project, faculty advice, for their input and suggestions.

GENERAL INDEX

	Pag.
ABSTRACT	3
RESUMEN	4
ACKNOWLEDGEMENTS	7
INDEX OF TABLES	11
INDEX OF APPENDICES	12
INTRODUCTION	13
LITERATURE REVIEW	16
Clinical picture of myotonic dystrophy (DM):	16
Neuropsychological symptoms of DM1:	16
Neuropathology of DM1:.....	17
Genetics of DM:.....	17
Differences between DM1 and DM2.....	18
Molecular pathogenesis of DM1: the toxic RNA hypothesis	19
MBNL Sequestration:	21
CELF upregulation:	21
Missplicing of TAU:.....	22
Missplicing of NMDAR1:	22
Missplicing in APP:	23
Others missplicing genes:	23
The DMSXL mice: a transgenic model of RNA toxicity	23
Preliminary results: investigation of disease targets in the CNS of a mouse model of DM1	25
Cell lines used to validate and complement the analysis of DMSXL transgenic mice. ..	26
Advantages and Limitations of cell lines.....	26
OBJETIVES	28
MATERIALS AND METHODS:	29
1. PLASMID TEST:	29
2. CELL CULTURE AND TRANSFECTION:	31
3. FOCI DETECTION:	31
4. RNA EXTRACTION:	32
5. RT-PCR FOR CANDIDATE GENES:	33
6. PROTEIN EXTRACTION:.....	33
7. WESTERN BLOT:	34
RESULTS	35
1. EVALUATION OF THE SIZES OF THE PLASMIDS:	35
2. VALIDATION OF RNA TOXICITY IN DM1 CELL CULTURE SYSTEM:	36
2.1 Accumulation of foci in transfected cells:.....	36
3. DEREGULACION OF ALTERNATIVE SPLICING IN DM1 CELL MODELS	38
3.1. RNA extraction and cDNA synthesis:	38
3.2. MBNL1	39
3.3 MBNL2:	41
3.4 INSR:.....	42
3.5 APP:.....	43
4. EXPRESSION DEFECT	45

4.1 SK3:	45
5. PROTEIN EXPRESSION	47
5.1. CELF1:	47
RESULTS DISCUSSION	49
RECOMMENDATIONS	52
BIBLIOGRAPHY	53
APPENDIX SECTION	59
1. PLASMID STRUCTURES:	59
2. CELL CULTURE MEDIUM COMPOSITION:	59
3. PCR 300 PROTOCOL:.....	60
4. OLIGO'S SEQUENCES AND CONDITIONS:	61
5. PROTEIN DETAILS:.....	62
6. ANTIBODIES SOLUTIONS USED BY WESTERN BLOT:.....	63
7. RNA EXTRACTION AND HOMOGENIZATION:	63
8. OLIGOS TESTED GELS PICTURES FROM THE QUALITATIVE RESULTS:....	64
9. OLIGOS TESTED GELS PICTURES FROM THE QUANTITATIVE RESULTS:..	65
10. HOJA DE INFORMACIÓN.....	68

INDEX OF FIGURES

INDEX OF FIGURES

Number	Title	Page
1.	Digestion of the DMPKS and DT960 plasmid DNA obtained from transformed bacteria.	36
2.	Foci expression in transfected cell lines SH-SY5Y (A), T98-G (B) and HeLa (C) cells.....	36
3.	Quantification of CUG-containing RNA foci in SH-SY5Y (A), T98-G (B) and HeLa (C) cells transfected with DT960 construct.	37
4.	<i>MBNL1</i> PCR to evaluate the missplicing in the exon 7.....	39
5.	Quantitative analyses of <i>MBNL1</i> exon 7 missplicing.....	40
6.	<i>MBNL2</i> PCR to evaluate the missplicing in the exon 7.....	41
7.	Quantitative analyses of <i>MBNL2</i> exon 7 missplicing.....	42
8.	Quantitative analyses of <i>INSR</i> exon 11 missplicing.....	42
9.	Quantitative analyses of <i>APP</i> exon 8 missplicing.	43
10.	<i>CaMK2γ</i> PCR to evaluate the missplicing in the exon 13.	44
11.	Quantitative analyses of <i>CaMK2γ</i> exon 13 alternative splicing.	45
12.	Semi-quantitative RT-PCR analysis of <i>SK3</i> transcript in SH-SY5Y cells under different conditions	46
13.	Semi-Quantitative RT-PCR analyses of the expression of <i>SK3</i>	47
14.	Western Blot analyses of CELF1 expression	48
15.	Quantitative analyses of the CELF1 expression	48
16.	Plasmids used to transfect SH-SY5Y, T98-G and HeLa cell lines.....	59
17.	Extracted RNA from SH-SY5Y, T98-G and HeLa transfected cell lines with the plasmids DMPKS and DT960..	63
18.	Example of β -actin PCR, using in the homogenization of the cDNA samples of transfected T98-G (A) and SH-SY5Y (B) cell lines	63
19.	Qualitative gels data for check the splicing defect and the expression. These genes did not show expression, splicing defect or right sizes bands	64
20.	Qualitative gels data for check the splicing defect and the expression in transfected SH-SY5Y cells..	65
21.	Qualitative gels data for check the splicing defect and the expression in transfected T98-G cells.....	66
22.	Qualitative gels data for check the splicing defect and the expression in transfected HeLa cells.....	67

INDEX OF TABLES

INDEX OF TABLES

Number	Title	Page
1.	PCR 300 profile.	60
2.	PCR's oligonucleotides primers, sequences and conditions.	61
3.	Gel components concentration.	62
4.	Buffer Solutions components.	62
5.	Specifications of the Antibodies.	63

INDEX OF APPENDICES

INDEX OF APPENDICES

Number	Title	Page
<u>1.</u>	PLASMID STRUCTURES:	59
<u>2.</u>	CELL CULTURE MEDIUM COMPOSITION:	59
<u>3.</u>	PCR 300 PROTOCOL:	60
<u>4.</u>	OLIGO'S SEQUENCES AND CONDITIONS:	61
<u>5.</u>	PROTEIN DETAILS:	62
<u>6.</u>	ANTIBODIES SOLUTIONS USED BY WESTERN BLOT:	63
<u>7.</u>	RNA EXTRACTION AND HOMOGENIZATION:	63
<u>8.</u>	OLIGOS TESTED GELS PICTURES FROM THE QUALITATIVE RESULTS:	64
<u>9.</u>	OLIGOS TESTED GELS PICTURES FROM THE QUANTITATIVE RESULTS:	65
<u>10.</u>	HOJA DE INFORMACIÓN.....	68

INTRODUCTION

For a long time, the human genome was considered as an intrinsically stable entity. At present we know that our genome contains many unstable elements consisting of tandem repetitive elements that range in length from two to several thousand of nucleotides (Bermudez & Cisneros, 2008).

Triplets repeat mutations were discovered in 1991, and since that date they have been identified as the cause of multiple human diseases. The repeats are polymorphic in the normal, non-affected population, and they are believed to have no phenotypic consequences until reaching a certain pathogenic length, characteristic of each gene. Actually, 16 human neurological and neuromuscular disorders are known to be caused by the expansion of (CUG)_n, (CGG)_n, (CCG)_n, (GAA)_n, and (CAG)_n trinucleotide repeats in single genes. These diseases include myotonic dystrophy type 1, fragile X syndrome, Friedreich ataxia, spinocerebellar ataxias and Huntington disease. Their common feature is genetic anticipation, whereby the age of disease onset decreases in successive generations of an affected family (Bermudez & Cisneros, 2008; Kohwi, 2004).

Myotonic dystrophy (DM) is one of the most variable human disorders and the most common adult onset muscular dystrophy, affecting mainly skeletal muscle, heart, and the central nervous system (CNS). DM worldwide prevalence is estimated to be ~1/8,000. Mutations in two genes cause DM. DM type 1 (DM1) is caused by the expansion of a CTG repeat within the 3' untranslated region of the *DMPK* (myotonic dystrophy protein kinase) gene; and DM type 2 (DM2) is caused by a CCTG repeat expansion in intron 1 of the *ZNF9* (zinc finger protein in gene 9). The pathogenic mechanism involves a novel RNA gain of function in which repeat-containing transcripts from the expanded *DMPK* or *ZNF9* allele accumulate in nuclei and alter the functions and distribution of RNA binding proteins involved in regulating alternative splicing, mRNA transcription and translation (Ranum & Cooper, 2006).

DM1 research initially concentrated on muscle and cardiac pathology, while the neurological symptoms were somehow overlooked and neglected. This view has changed dramatically over the last few years. Research scientists, medical doctors and other health professionals have recognized the heavy impact of the disease on the CNS and on the patient's quality of life. The congenital form of the disease is characterized by a severe mental retardation. Some of the symptoms like hypersomnia (excessive daytime sleepiness), learning problems, personality disturbances, reduced initiative and social avoidance have all been reported and considered as highly debilitating by adult and juvenile DM1 patients (Meola & Sansone, 2007; Bermudez & Cisneros, 2008; Morales *et al.*, 2001).

Although circumstantial data have supported a role of *trans*-dominant toxic RNA transcripts in DM1 brain dysfunction, the molecular pathophysiology of the neurological symptoms remains elusive. The establishment of a functional link between trinucleotide repeat expansion, expression and accumulation of toxic RNA molecules, cell dysfunction and the development of neurological symptoms will provide scientific advances in the understanding of the mechanisms of DM and other repeat expansion disorders.

The INSERM U781 host laboratory takes advantage of transgenic mice to investigate the mechanisms of DM. Transgenic DM mice express an expanded *DMPK* gene in multiple tissues, such as the CNS. These animals recreate important aspects of the DM1 repeat dynamics and phenotype, notably brain abnormalities, and provide a unique resource to investigate the far-reaching biological consequences of the *trans*-acting pathogenic expansion in the CNS. Preliminary evidence suggests deregulation of calcium metabolism in the CNS of DM transgenic mice in response to the expression of toxic CUG-containing transcripts. Calcium homeostasis plays an important role in the CNS, so calcium abnormalities might have important physiological consequences, and contribute to the neurological manifestations of the disease.

The advances in biotechnology have resulted in the development of transgenic mouse models of complex human diseases, such as DM. Indeed, more than 20 DM mouse models are currently available. The study of multiple transgenic lines over the years has greatly contributed to dissect the molecular mechanisms behind the onset of symptoms, and to put forward a new disease mechanism based on the toxicity of non-coding RNAs. Currently, the new challenge for Biotechnology is to make use of these animals to identify targets for therapeutic intervention. The understanding of molecular mechanisms of disease will help design and test new and efficient methods of therapy. New therapies might be first tested in transgenic animal models generated by biotechnological methods and which recreate key features of the disease. The on-going research will contribute to the establishment of a rational basis for the development of future therapeutic assays.

The project described and discussed in this report, addresses the molecular and cellular bases of the neurological dysfunction reported in DM1 patients, focusing in possible alterations in calcium metabolism in brain cells (neuroblastoma and glioblastoma).

LITERATURE REVIEW

Clinical picture of myotonic dystrophy (DM):

DM is the most common form of adult muscular dystrophy; including two genetically distinct but clinically similar disease forms. DM1 accounts for the majority of DM cases (traditionally >95%). The remaining 5% are usually attributed to myotonic dystrophy type 2 (DM2). DM1 is a truly multisystemic disorder, showing great variability of disease manifestations and age of onset. The adult onset form of DM1 typically shows progressive muscle weakness and wasting, myotonia, presenile cataracts, cardio-respiratory problems, hypersomnia and hyperinsulinism. Behavioural changes and cognitive dysfunction are also frequent. The progressive nature of the disease often leads to significant disability. The more severe congenital form of DM1 is characterized by general hypotonia and respiratory distress at birth, as well as delayed motor development and severe mental retardation (Harper, 2001). Currently there is no satisfactory treatment.

Neuropsychological symptoms of DM1:

Given the prominent muscle weakness and myotonia (slow relaxation of the muscles after voluntary contraction), DM was initially considered a muscle disease. However, DM is a multisystemic disease affecting virtually all tissues and organs, including the CNS. Hypersomnia, cognitive deficits and learning difficulties, reduced initiative, anhedonia, as well as avoidant, obsessive-compulsive, and passive-aggressive personalities have been reported to a variable extent (Harper, 2001). The marked impairment of the cognitive control of behaviour suggests mental dysfunction (Meola *et al.*, 2003). Congenital patients suffer from severe mental retardation. Neuropsychological symptoms are usually milder in DM2 (Meola & Sansone, 2007). DM1 patients, in particular suffering from the juvenile form of the disease, present cognitive impairment in all measures of general intelligence and verbal fluency and particularly frontal, executive, visuospatial, arithmetic, and attention ability deficits (Abe *et al.*, 1994; Modoni *et al.*, 2004; Winblad *et al.*, 2006).

Neuropathology of DM1:

Neuropathology studies revealed a number of findings associated with DM1. Cell loss in the cerebral cortex, neuronal inclusion bodies (mostly in the thalamus, caudate and other brainstem nuclei), decreased myelin sheathing, and increased neurofibrillary tangles. Neurofibrillary tangles are present in the limbic system and/or the brainstem, hippocampus, entorhinal cortex, and temporal areas. Corpus callosum atrophy was described in association with sleep perturbation, one of the most distinctive DM1 features. No significant decrease in the volume of parietal cortex has been found in DM1 patients. No senile plaques or amyloid beta deposits have been detected so far. The increased levels of phosphocreatine, choline, and myoinositol found in DM1 patients suggest increased glial content and cell membrane abnormalities in brain (Bermudez & Cisneros, 2008). Recent imaging studies will help elucidating the relationship between brain structural abnormalities, metabolism abnormalities and DM neuropsychological manifestations (Romeo *et al.*, 2010; Wozniak *et al.*, 2011).

Despite circumstantial evidence suggest on-going and progressive CNS dysfunction DM1, little is known about the mechanistic link connecting DNA mutation, to molecular abnormalities, histopathology, dysfunctional pathways and development of neuropsychological symptoms.

Genetics of DM:

DM1 is caused by the autosomal dominant expansion of an unstable CTG repeat in the 3'UTR of the *DM protein kinase (DMPK)* gene (Brook *et al.*, 1992). There is a broad correlation between repeat size and the age of onset and the severity of symptoms. The repeat normally ranges between 5–37 CTG in the non-affected population (Tsilfidis *et al.*, 1992). Individuals with 50-100 CTG repeats present late-onset DM1, mainly characterized by premature cataracts. Repeat sizes of 100-500 CTG repeats are associated with the classical adult onset of DM1, which presents myotonia, muscle weakness, cardiac conduction defects, endocrine dysfunction, cognitive decline, behavioural changes and hypersomnia. The most severe form of the disease, the congenital form, is developed by individuals that inherit more than 500, up to >4000 CTG repeats (Harper *et al.*, 2001). The boundaries are not rigid, and there might be some overlapping of repeat lengths between different forms of the disease.

The expanded CTG sequence is unstable and tends to expand in size as it is transmitted vertically within a family (from one generation to the next). For this reason, intergenerational, expansion-biased, trinucleotide repeat instability serves as the molecular explanation of the phenomenon of anticipation, whereby disease severity increases and age of onset decreases in successive generations of a DM1 family (Harper *et al.*, 1992).

The CTG repeat is also unstable in somatic tissues. The somatic instability of DM1 CTG repeats has been reported in a wide range of human tissues. Somatic expansion in DM1 is clearly age dependent, with longer average DM1 repeat lengths and broader ranges of variability observed in older patients. Somatic mosaicism analysis have revealed a gradual increase in allele length and variation with age, demonstrating that expansion is mediated by multiple small length changes in a highly deterministic pathway, which most certainly contributes to phenotypic variability and disease progression (Gomes-Pereira & Monckton, 2006).

The DM2 is caused by the expansion of a CCTG tetranucleotide in the first intron of *ZNF9* gene (Liquori *et al.*, 2001).

Differences between DM1 and DM2

DM2 is generally milder than DM1 and lacks a severe congenital form. The muscle histopathology observed in DM1 is also seen in DM2. The main difference between DM1 and DM2 consists in the muscle groups mainly affected in each disease: DM1 affects mainly distal muscles, while DM2 affects primarily proximal muscles. The non-muscle manifestation, cataracts, cardiac arrhythmias, abnormalities of the cerebral hemispheric white matter and hypogonadism are presented in both diseases. The *in vitro* and cell culture work have suggested the possibility that methylation occurring at the DM1 locus in congenital cases, may increase *DMPK* expression by activating the nearby *SIX5* enhancer, a model consistent with the idea that increased expression of CUG expansion transcripts in congenital DM1 may cause the more severe phenotype than in DM2 (Mankodi *et al.*, 2001; Ramun & Cooper, 2006).

The parallel between DM1 and DM2 is explained by a common mechanism of pathogenesis, mediated by a dominant gain of function of expanded mRNAs (Ranum & Cooper, 2006).

Molecular pathogenesis of DM1: the toxic RNA hypothesis

The development of transgenic mice pointed to a novel disease mechanism mediated by toxic RNA repeats. Expanded *DMPK* transcripts accumulate in the nuclei of DM1 cells, interfering with at least two protein families that act antagonistically on the regulation of alternative splicing throughout development: the muscleblind-like (MBNL) and CUGBP/Elav-like family (CELF) proteins: MBNL1 function is lost due to sequestration by ribonuclear aggregates or foci, and CELF1 (or CUG-binding protein 1, CUGBP1) is upregulated. MBNL1 sequestration and CELF1 upregulation recreate a foetal scenario, resulting in aberrant expression of embryonic splicing profiles of MBNL1- and/or CELF1-regulated transcripts in adult skeletal muscle and heart. *CLCN1* chloride channel missplicing in skeletal muscle results in myotonia, whereas abnormal splicing of the *insulin receptor* may contribute to insulin resistance (Ranum & Cooper, 2006). More than 20 alternative splicing events in more than 20 different genes are misregulated in different DM1 tissues, contributing to the multisystemic nature of DM (Osborne, 2006). It is likely that many more remain to be identified. Nevertheless, DM molecular pathogenesis may go beyond spliceopathy and involve deregulated gene expression (Ebralidze *et al.*, 2004; Osborne *et al.*, 2009; Botta *et al.*, 2007).

Splicing Abnormalities:

Alternative splicing provides a regulatory mechanism by which vertebrates can regulate the expression of tissue-specific or developmental stage-specific protein isoforms. RNA binding proteins, which regulate the alternative splicing, bind to specific sequence elements in the pre-mRNA to enhance or repress inclusion of alternative exons. Deregulation of alternative splicing can cause the expression of inappropriate isoforms leading to human disease. Missplicing in DM1 is limited to specific pre-mRNA targets, rather than affecting splicing in general. In all cases the expression of foetal protein isoforms that are inappropriate for adult tissues have been observed in DM1 patients. Misspliced genes in skeletal and cardiac muscles include cardiac troponin T (*TNNT2*), insulin receptor (*IR*), muscle-specific chloride channel (*CLCN1*), myotubularin-related protein 1 (*MTMR1*), fast skeletal troponin T (*TNNT3*), ryanodine receptor (*RyR*), and sarcoplasmic/endoplasmic reticulum calcium ATPase (*SERCA1*) (Osborne *et al.*, 2009). Two splicing events have been associated with muscle symptoms: insulin resistance and myotonia observed in DM1 correlate with disruption of splicing of *IR* and *CLCN1*, respectively (Osborne *et al.*, 2009). The physiological consequences of other splicing defects are not fully understood.

Some other genes are affected in DM1 brains: *TAU* (*MAPT*), N-methyl- D-aspartate receptor 1 (*NMDAR1*), and amyloid precursor protein (*APP*) (Jiang *et al.*, 2004). Nevertheless the impact of these abnormalities on brain dysfunction and contribution to DM1 neuropsychological manifestations requires further studies.

MBNL Sequestration:

Two different alternative splicing regulator families have been implicated in the DM molecular pathogenesis: MBNL and CELF proteins.

MBNL1 and MBNL2 (muscleblind-like proteins) are RNA binding proteins, mainly involved in the regulation of alternative splicing of pre-mRNA targets. MBNL1 and MBNL2 colocalize with DM1 and DM2 ribonuclear foci (Fardaei *et al.*, 2002). The role of MBNL1 loss of function in DM (due to protein sequestration) is corroborated by the phenotype observed of *Mbnl1* knock-out mice, which develop myotonia associated with splicing misregulation of *CLCN1*, and decreased expression of the chloride channel in skeletal muscle. In addition *Mbnl1* knock-out mice develop the same type of cataracts than DM1 patients (Kanadia *et al.*, 2003). In summary, MBNL1 sequestration by nuclear foci and subsequent loss of function is sufficient to generate some key features of the DM1 phenotype.

CELF upregulation:

CELF1 has been originally identified given its ability to bind CUG RNA repeats *in vitro* (Timchenko *et al.*, 1996). Six CELF genes have been identified in humans. All six CELF proteins have been shown to regulate pre-mRNA alternative splicing and two (CELF1 and CELF2) have cytoplasmic RNA processing functions (Barreau *et al.*, 2006). CELF1, as well as other CELF family members, regulates alternative splicing of at least three of the pre-mRNAs that are mis-regulated in DM1 striated muscle: cardiac troponin T (cTNT), insulin receptor (IR) and *CLCN1*. In brain, CELF proteins regulate the alternative splicing of *TAU* and *NMDAR1* mRNAs (pre-mRNAs that displayed missplicing in DM1 cortical neurons) (Barreau *et al.*, 2006).

In DM1 tissues, CELF1 is hyperphosphorylated by PKC, resulting in increased stability and subsequent upregulation (Kuyumcu-Martinez *et al.*, 2007). CELF1 upregulation *per se*, is sufficient to induce missplicing in the heart and skeletal muscle of transgenic mice overexpressing this protein (Koshelev *et al.*, 2010; Ward *et al.*, 2010). CELF1 is therefore a central player in DM1 pathology. The role of other CELF members in the mechanisms of DM1 is less clear. Currently it is not known to which extent CELF deregulation contributes to DM2 or brain dysfunction (in both DM1 and DM2).

RNA missplicing in the CNS: findings and implications

The analysis of post-mortem DM1 brains has revealed defects in the alternative splicing of some genes (Jiang *et al.*, 2004). Nevertheless the implications of these molecular abnormalities to DM1 neuropathophysiology are not fully understood.

Missplicing of TAU:

TAU (MAPT) protein belongs to the microtubule associated family, and it is essentially expressed in neurons, where its main function is to regulate the microtubule network. This protein plays an important role maintaining the stability of the neuronal cytoskeleton through the interaction with microtubules. TAU is involved in the pathogenesis of neurodegenerative disorders. In adult human brain the alternative splicing of exons 2, 3 and 10 transcripts give six TAU isoforms. The DM1 CTG repeat expansion alters *TAU* alternative splicing, probably affecting TAU protein binding to microtubule or affecting the post transcriptional maturation of *TAU* pre-mRNA. Although it is unclear how *TAU* missplicing is related to DM1 neuronal dysfunction, neurofibrillary tangles containing TAU have been described in DM1 patients (Bermudez & Cisneros, 2008).

Missplicing of NMDAR1:

N-methyl- D-aspartate receptor 1 (NMDAR1) is required for normal long term potentiation in the hippocampus as well as in learning processes. An increased inclusion of *NMDAR1* exon 5 has been observed in the temporal cortex of DM1 patients (Jiang *et al.*, 2004). Inclusion of this exon influences pharmacological behaviour, gating, and subcellular distributions (somatic rather than somato-dendritic expression) of this receptor (Zukin *et al.*, 1995). It has been suggested that exon 5 altered splicing may account for the memory impairment observed in DM1 patients. It is thought that CELF proteins participate in the regulation of exon 5 alternative splicing of *NMDAR1* mRNA. Nevertheless, it is still unclear how the DM1 mutant transcripts could interfere with this *NMDAR1* missplicing in brain and explains some neurological manifestations of the disease process. No colocalization has been observed between CELF proteins and DM1 associated RNA foci in neurons (Jiang *et al.*, 2004).

Missplicing in APP:

The APP may function as a “cell surface receptor”, controlling intracellular signalling pathways. APP and its derivatives have been implicated in the regulation of G-protein coupling, calcium homeostasis, neurite outgrowth and adhesion (Linde *et al.*, 2011). It is known that alternative splicing generates three different *APP* splicing variants. An increased expression of *APP* foetal splice isoform lacking exon 7 in the temporal cortex of DM1 patients has been reported (Jiang *et al.*, 2004), yet no information is available about the functional significance of this splicing alteration in DM1 (Bermudez & Cisneros, 2008).

Others missplicing genes:

Has been proved that *NMDAR*, *TAU* and *APP* genes have an obvious splicing defect in brain human samples, based on this is probable to evaluate the possibility to find others missplicing sites or defects and changes in the expression levels of genes in brain, associated with the CNS in DM1 which have not been described yet.

The DMSXL mice: a transgenic model of RNA toxicity

The mouse presents an ideal animal model to assess repeat biology *in vivo*, given its relatively short generation time, genetic similarity to humans and ability to be genetically manipulated. Transgenic mice have been generated to provide *in vivo* models to study repeat instability in the germ line and during somatic development, as well as to provide models of disease pathogenesis. These mouse models have proved to be an excellent tool to investigate the molecular mechanisms mediating simple repeat expansion. Mouse models have been generated to explore the mechanisms to DM molecular pathogenesis (Wansink & Wieringa, 2003).

In the host laboratory, and in order to dissect the pathophysiology associated with toxic RNA transcripts, a large genomic fragment of the human DM1 locus, comprising the *DMPK* gene and a variable number of CTG repeats, was inserted in the mouse genome. Transgenic lines were created carrying control 20-CTG tracts (DM20 lines) or disease-associated 320-CTG sequences (DM300 lines). The DM300 mice recreate nuclear RNA foci accumulation, as well as histological and electrophysiological abnormalities, including myotonia, atrophy and fibrosis of skeletal muscle. In the CNS, DM300 exhibit TAU hyperphosphorylation and misdistribution of TAU protein isoforms (Seznec *et al.*, 2001), mirror the tauopathy described in DM1 patients (Sergeant *et al.*, 2001). The dramatic expansion based intergenerational repeat instability resulted in mice carrying more than 1000 CTG repeats (DMSXL mice). These animals show a more severe phenotype, including extensive foci accumulation and splicing defects of relevant genes in the CNS, and represent an excellent tool to unravel the neuropathogenesis of DM1 (Gomes-Pereira *et al.*, 2007).

The DMSXL mice of the host laboratory represent the only animal model that recreates both trinucleotide repeat instability and a phenotype associated with DM1, notably brain specific abnormalities. Currently, no other DM1 mouse model has recreated molecular or physiological abnormalities in the CNS. Therefore, these animals present the best available tool to decipher the molecular and cellular aspects of DM1 neuropathology and to test future therapeutic strategies.

Preliminary results: investigation of disease targets in the CNS of a mouse model of DM1

In order to identify new proteins and pathways affected by the trinucleotide repeat expansion in the CNS of transgenic mice, the host laboratory has used a global proteomic approach. The comparison of the proteomic profiles of frontal cortex and brainstem between the expansion line available at the time of the analysis (DM300) and the short repeat line (DM20) resulted in the identification of ~30 candidate target proteins, which appear to be affected by the CTG expansion. The proteomic approach reveals not only differences in the expression levels of proteins targeted by the mutation, but also disease associated post transcriptional and/or post translational modifications (such as differences in phosphorylation). The proteomic analysis is currently being extended to DMSXL mice (carrying more than ~1000 CTG, up to ~1800 CTG), in order to identify molecular abnormalities triggered by larger repeat expansions, which might have been disregarded in DM300 mice previously used (carrying ~600 CTG). Some of the proteins identified are involved in the regulation of calcium metabolism and homeostasis, suggesting that the CTG repeat expansion may affect calcium signalling pathways in the CNS. In further support of this hypothesis, other research groups have performed microarray expression analysis of skeletal muscle collected from DM1 patients and other transgenic mouse models, and found expression abnormalities in genes involved in calcium homeostasis (Botta *et al.*, 2007; Osborne *et al.*, 2009).

Cell lines used to validate and complement the analysis of DMSXL transgenic mice.

For the development of this project three human cell lines were chosen: SH-SY5Y, T98-G (both from brain) and HeLa (epithelium). The following information was taken from www.lgcstandards-atcc.org

- **SH-SY5Y** is a neuron cell line obtained from human neuroblastoma, which provides a neuronal cell system in culture to study the molecular and cellular effects of the CTG repeat expansion.
- **T98-G** is an astrocyte cell line derived from a brain glioblastoma, which retains important glial properties and is therefore used to model the pathophysiological consequences of the DM1 mutation in astrocytes.
- **HeLa cells** are epithelium cells derived from the adenocarcinoma cervix. These cells have been selected given that in contrast with neurons and astrocytes, HeLa cells are easy to transfect by standard procedures, and serve as a transfection control in these experiments.

Advantages and Limitations of cell lines

The use of cell lines could be an option to develop some investigation that are no possible on human or mouse tissue samples. They present some advantages, like the possibility to control the culture conditions (as pH, temperature, osmotic pressure, O₂ and CO₂ tension) using the appropriated mediums, serums and constituents. Importantly, cell lines are homogeneous populations, which self-replicate and provide a continuous source of material. *In vitro* cultures reduce expenses, and have less legal, moral and ethical requirements, when compared to animal experiments. The development of histotypic and organotypic models also increases the accuracy of *in vivo* modelling. However, there are also some limitations: occasionally the dedifferentiation of some cell lines is required to get a suitable model for obtaining appropriated results, sometimes it is difficult to relate the cultured cells to functional cells in the tissue from which they were derived and also genetic instability is a big problem with many continuous cell lines, as a result of their unstable aneuploidy chromosomal constitution. Even with short-term cultures of untransformed cells, heterogeneity in growth rate and the capacity to differentiate within the population can produce variability (Freshney, 2005).

The transfection of the neurons and astrocytes is very important to confirm the previous results obtained in the transgenic mice supporting the idea that molecular abnormalities detected in mice are the consequence of the expression of toxic CTG repeats. Together will be useful to provide a cell model system that is easy to manipulate and in which it is possible to test the functional consequences of the molecular abnormalities in calcium metabolism.

In order to study the calcium metabolism and follow the validation of RNA toxicity, was used a cell culture model system of DM1 transfected cells with 960 CTG repeats (neuron and astrocyte). In addition, HeLa cell lines with a DMPK construct containing 960 CTG repeat, were used. Epithelium cells worked as a control for transfection, knowing that this cell line is easier to transfect than neurons and astrocytes. A construct containing no CTG repeats was used as control to evaluate if the presence of the DMPK gene without repeats could generate some defect in the transfected cells.

OBJETIVES

GENERAL OBJETIVE:

- To establish and characterize a brain cell culture model system of myotonic dystrophy type 1 to study calcium metabolism deregulation and homeostasis.

SPECIFIC OBJETIVES:

1. To detect the presence and the right sizes of the CTG repeat expansion in the plasmid DT960 and compare with DMPKS plasmid as control.
2. Once the right CTG repeat size were confirmed, transfected cell lines were used to identify the presence and the quantity of foci in transfected SH-SY5Y (neurons), T98-G (astrocytes) and HeLa (epithelium) cells lines.
3. To study the impact of the 960 expanded CTG repeats on the alternative splicing of candidate genes in SH-SY5Y (neurons), T98-G (astrocytes) and HeLa (epithelium) cells lines transfected with expanded and control DMPK construct.
4. To measure the expression levels of candidate genes SH-SY5Y, T98-G and HeLa cells lines transfected with DMPK, containing or not the CTG repeat expansion.
5. To investigate the steady levels of the candidate proteins in the population cells lines (SH-SY5Y, T98-G and HeLa), transfected with expanded and control DMPK construct.

MATERIALS AND METHODS:

1. PLASMID TEST:

Two plasmids were used to transfect cells:

- The DT960 plasmid contains a fragment of the human *DMPK* gene carrying 960 CTG repeats in the 3'UTR;
- The DMPKS plasmid contains a fragment of the human *DMPK* gene carrying no CTG repeats in the 3'UTR.

Escherichia coli bacteria were transformed with DT960 (bacteria variety Sure 2) and DMPKS (bacteria wild type) plasmids using the TRANSFORMATION PROTOCOL FOR DT960 (AMPICILLIN RESISTANT) (WITH SURE 2 SUPERCOMPONENT CELLS) from Agilent Technologies 200152, the culture medium used was SOC medium for the bacteria transformation liquid culture.

The DNA was extracted from the transformed colonies using the protocol 2, PREPARATION OF PLASMID DNA BY ALKALINE LYSIS WITH SDS: MIDIPREPARATON, from the Molecular Cloning book Volume I from Sambrook and Russell Book (2001).

To evaluate the presence of the plasmids in the bacteria, the PCR 300 (2,5 µl of Buffer 10X from Thermo Scientific, 1 µl of primer 101, 1 µl of primer 102 both primers from Eurogentec Company, 0,04 µl of Taq PFU from Thermo Scientific, 1 µl of DNAC and 20,46 µl of water) was run in the Applied Biosystem PCR Thermo Cyclor Version 2.09 following the program attached in the Table 1 from the Appendix. This PCR was created to evaluate the right size of the plasmids. The bands were checked on a 0,7 % agarose gel, run at 100 V during 1 hour. The PCR samples were prepared with 5 µl of bromophenol blue. Later, 10 µl of sample and 10 µl of the Invitrogen ladders (100 bp DNA ladder and 250 bp DNA ladder) were loaded. The gel was analysed by the BioRad Gel Doc System using the Quality One Software 4.6.3.

To reconfirm that the plasmids had the right sizes, a digestion of the DNA plasmids (DMPKS and DT 960) was developed, the samples were prepared using 2 µl of buffer 10X BamHI and 1 µl of enzyme BamHI (both reagents from the company Bio Labs). The concentration of the DNA was measured with the Nanodrop spectrophotometer 1000 from Thermo Scientific (the quantity of water was regulated in based of the DNA concentration to obtain a 20 µl as final volume). To check the result a 0,7 % agarose gel was run at 120 V for 2 hours. The samples were mixed with 5 µl of orange color 10X and then loaded in the gel. To check the right sizes of the bands the 100 bp DNA ladder, 250 bp DNA ladder and Hind III ladders from Invitrogen were used. The gel was analysed by the BioRad Gel Doc Machine using the Quality One Software 4.6.3.

To prepare a midi prep the bacteria were cultured in Falcon tubes with 5 ml of LB medium supplemented with 5 µl of antibiotic (Kanamycine for DMPKS and Ampiciline for DT960) during 7 hours, at 275 rpm and 37 °C. Then 400 µl of the colonies were taken from the Falcon tube and transferred to an 1 L Erlenmeyer with 400 ml of LB medium and 400 µl of antibiotic, then the midi prep was incubated at 37 °C and 275 rpm overnight (approximately 14,5 hours).

The DNA was extracted from the bacteria colonies using the protocol PLASMID OR COSMID DNA PURIFICATION USING HISPEED PLASMID MIDI AND MAXI KITS from Qiagen. The bacteria colonies were centrifuged at 4500 rpm and 20 minutes at 8 °C. To elute the DNA 10 ml of buffer QF was added, and the DNA was precipitated adding 7 ml of isopropanol at room temperature.

To evaluate the right sizes from the DNA plasmids extracted with the midi prep protocol, a digestion was performed, using the same conditions explained before. One sample of DT960 and other one of DMPKS were used as controls. A 0,8% agarose gel (supplemented with etidium bromide) was used with the same conditions that the first digestion. The gel was analysed using the BioRad Gel Doc System using the Quality One Software 4.6.3.

2. CELL CULTURE AND TRANSFECTION:

The cell lines (SH-SY5Y, T98-G and HeLa) were cultured in DMEM medium supplied with Foetal Bovine Serum, Penicillin and Streptomycin. For T98-G medium also had Gentamycin. In each culture, the cells were washed with DPBS and raised from the plates (diameter size 10 cm) with Trypsine 0.35% and incubated during 5 min at 37 °C. The Trypsine was not removed. In each plate was added 4 ml of medium and transferred in new 15 ml Falcon tubes. The tubes were centrifuged at 800 rpm during 5 minutes. To suspend the pellet 1 ml of new medium was added. Finally 200 µl for SH-SY5Y, 50 µl for T98-G and 250 µl for HeLa were plated in new dishes with 10 ml of fresh medium. This protocol was developed in three repeats for each cell type. All the cultures were incubated at 37 °C with 5% of CO₂ and humidity (the details of the culture media are attached on the section 1 CELL CULTURE MEDIA COMPOSITION in the Appendix).

The cell lines were transfected with DMPKS and DT960 plasmids, the TRANFECTION BY USING LIPOFECTAMINE LTX AND PLUS-REAGENTS PROTOCOL from Invitrogen Company was used to develop the transfection step.

3. FOCI DETECTION:

To detect the presence and the quantity of nuclear RNA foci in the transfected cell lines (SH-SY5Y, T98-G and HeLa) a fluorescent *in situ* hybridization (FISH) was developed. The standard protocol IN SITU HIBRIDIZATION FROZEN MUSCLE TISSUE with the (CAG)₅ probe was used. The cell counting was done manually using the Fluorescent Microscope Axioplan 2 to detect the foci and the software Qcapture Pro Fluoresce was used to take the pictures.

4. RNA EXTRACTION:

The RNA was extracted from the transfected cell lines with the EXTRACTION RNA WITH THE KIT TRIZOL MORE RNA PURIFICATION KIT FOR CELLS from Invitrogen protocol. In the section of binding, washing and elution: the Buffer I was added, the samples were centrifuged at 12 000 rpm during 15 seconds at room temperature, the flow was discarded, the DNase was added and incubated during 15 seconds, the Buffer I was added again and the samples were centrifuged at 12 000 rpm during 15 seconds at room temperature, the flow was removed and the Buffer II with ethanol was added. The samples were centrifuged at 12 000 rpm, for 15 seconds at room temperature, the flow was discarded and Buffer II with ethanol was added, the samples were centrifuged at 12 000 rpm during 1 minute at room temperature. The membrane tubes were transferred into 1,5 ml collect tubes and the RNase-Free water was added, the samples were incubated for 10 minutes and centrifuged for 2 minutes at 12 000 rpm at room temperature. The samples were run in 1% agarose gel (supplement with Etidium Bromure). The samples were prepared with 3 µl of 5X orange, 6 µl water and 1µl RNA extracted. The sizes were checked using the 250 bp DNA ladder from Invitrogen. The gel was run for 30 minutes at 100 V and was analysed by the BioRad Gel Doc System using the Quality One Software 4.6.3.

The RNA was synthesized in cDNA using the protocol cDNA SYNTHESIS BY REVERSE TRANSCRIPTION from Invitrogen Company. The cDNA samples were verified using β-actin primers provided for Eurogentec Company, the Applied Biosystems PCR Amplificator was programmed with 57 °C as annealing temperature and 26 cycles. The PCR products were loaded in 2% agarose gel, the sizes were checked using the 100 bp DNA ladder from Invitrogen and the gel was run for 20 minutes at 100 V, and then analysed by the BioRad Gel Doc System using the Quality One Software 4.6.3.

5. RT-PCR FOR CANDIDATE GENES:

The samples were homogenized relative to the intensity of the β -actin RT-PCR products to ensure that similar amounts of cDNA were used in each reaction.

To evaluate the splicing defect and the expression of different genes in DM1 the following genes were studied by semi-quantitative RT-PCR: *MBNL1*, *MBNL2*, *TAU*, *NMDAR1*, *CaMK2 β* , *CaMK2 δ* , *CaMK2 γ* , *RyR1*, *SK3*, *KCND3*, *CACNA2B*, *APP* and *INSR*. See the PCR oligonucleotide primer sequences and conditions in Table 2 of the Appendix Section.

Semi-quantitative analysis of splicing defects was performed on three replicates for each condition in the three cell types studied (SH-SY5Y, T98-G and HeLa cells). RT-PCR products were loaded and electrophoresed on agarose gels. The intensity of the bands was quantified with Quality One Software 4.6.3. (BioRad). Microsoft Excel was used to perform statistical analysis (t-student test).

6. PROTEIN EXTRACTION:

The cell cultures were harvested with 200 μ l of homogenization solution (1X complete mini (protease inhibitor), 0,5% w/v of CHAPS (from SIGMA Company), 100 nM okadaic acid (phosphate inhibitor), 1 mM orthovanadate (phosphate inhibitor) in RIPA 1X (from TERMO SCIENTIFIC Company). The lysate was shook slowly at 4°C for 5 minutes, and transferred into a 2 ml tube with metal beads and then shook 3 times for 15 seconds each at room temperature. Between each step the protein lysates were cooled down in ice for 3 minutes. The lysates were sonicated on ice at 50 of amplitude (5 times for 2 seconds each time). Then the samples were rotated during 1 hour at 4 °C, centrifuged at 12000 rpm for 5 minutes at 4°C. The quantity of protein was estimated with the BioRad PROTEIN ASSAY PROTOCOL.

Protein quality was verified by polyacrylamide gel electrophoresis. For the preparation of the samples each protein solution was denatured in SDS buffer and 5% β -mercaptoethanol at 95°C for 5 min. The proteins were subsequently electrophoresed through a 12% SDS polyacrilamide gel, and detected with Commassie Blue. For details on the preparation of the gels see Table 3 in the Appendix.

7. WESTERN BLOT:

For western blot analysis proteins were first electrophoresed through SDS polyacrylamide gels, as previously described. Proteins were then transferred onto PVDF membrane at 350 mA, for 2 hours in an ice container. At the end of the procedure, the membranes were stained with Ponceau staining solution to confirm protein transfer from gel onto membrane.

Membranes were blocked in 5% blotto solution with TBS-T 1X for 1 hour at room temperature, and then incubated with the primary antibody in 5% blotto at 4°C over night. The membrane was washed 3 times in TBS-T 1X and incubated with HRP-conjugated secondary antibody in 5% blotto for 1 hour at room temperature. Following 3 additional washes, western blot was revealed with Plus-ECL chemiluminiscent reagent (PerkinElmer). Membranes were stripped in stripping buffer at 50°C for 30 minutes prior to the incubation with additional antibodies. (See the details of the antibodies in the Table 5, in the appendix).

The proteins were quantified from the films by Quality One 4.6.3. (BioRad). Statistical analyses were performed with Microsoft Excel (t-student).

RESULTS

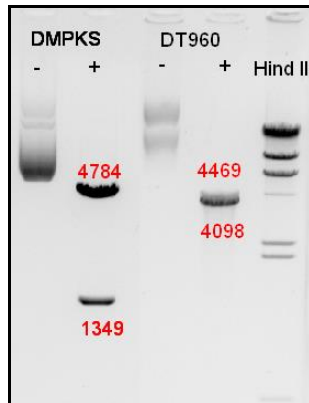
1. EVALUATION OF THE SIZES OF THE PLASMIDS:

In order to produce enough plasmid for the transfection experiments, DT960 and DMPKS plasmids were purified from large bacterial cultures (400 ml). While standard *E. coli* strains were transformed with DMPKS control constructs, *E. coli* (variety Sure 2) was used to amplify the repeat-containing DT960 plasmid, and avoid genetic instability and repeat size mutation.

A digestion of the extracted DNA from plasmid (DT960 and DMPKS) was performed to check the presence of the CTG repeats in the DT960 plasmid and absence of the CTG sequence in DMPKS control construct. Digested samples were loaded in a 0,8% agarose gel.

Figure 1 shows the expected sizes of the bands at 4784bp and 1349bp for the DMPKS plasmid, and 4469bp and 4098bp for DT960 plasmid, following digestion with DT960. The two digested bands were not fully resolved for the DT960 plasmid and they migrated together in the gel presented in Figure 1. However they have been observed independently in other experiments.

The sizes of the bands showed the restriction sites in where the enzyme BamHI cut the plasmids. The negative samples were used as a control for the no digestion of the samples.



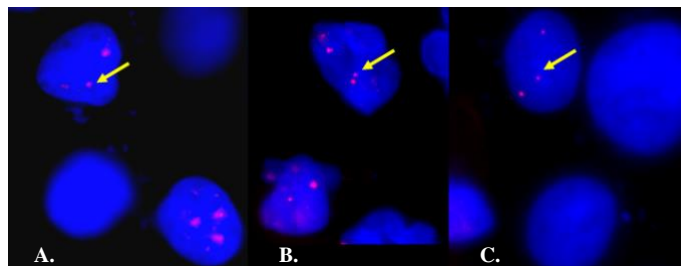
Quality One Software 4.6.3.

Figure 1. Digestion of the DMPKS and DT960 plasmid DNA obtained from transformed bacteria. The HindIII: lambda DNA digested with HindIII, the molecular weight ladder; (-: undigested plasmid; +: BamHI digested plasmid). DT960: expanded DMPK construct, two sizes expected (4469 base-pair (bp) and 4098bp). DMPKS: short DMPK construct, two sizes expected (4784bp and 1349 bp).

2. VALIDATION OF RNA TOXICITY IN DM1 CELL CULTURE SYSTEM:

2.1 Accumulation of foci in transfected cells:

The FISH was performed in order to identify the presence and quantity of foci in transfected with DT960 plasmid SH-SY5Y, T98-G and HeLa cells (figure 2). Foci are the result of the accumulation of expanded DMPK transcripts in the cell nuclei. Making use of the tool Fluorescent Microscope Axioplan 2 foci were identified and quantified in the different cell types.

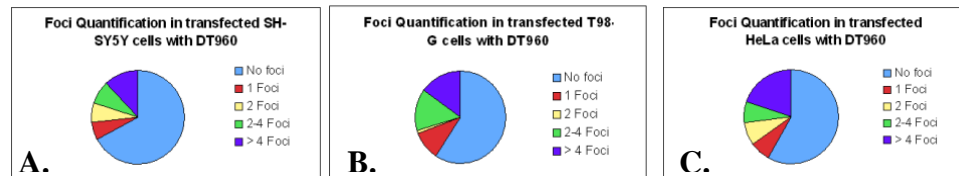


Qcapture Pro Fluoresce Software.

Figure 2. Foci expression in transfected cell lines SH-SY5Y (A), T98-G (B) and HeLa (C) cells. The arrow is focusing the example of foci in each picture, the blue (dapi): nuclei of the cells; red spot: toxic RNA (foci).

The three transfected population of cell lines presented RNA foci in the nuclei, characteristic of DM1, showing that transfected cells recreate RNA toxicity.

In order to quantify the accumulation of foci in different cell types, one hundred cells per cell line were carefully examined under the Fluorescent Microscope. The average of foci in each cell population was calculated, as well as the number of foci per individual cell.



Microsoft Excel Software

Figure 3. Quantification of CUG-containing RNA foci in SH-SY5Y (A), T98-G (B) and HeLa (C) cells transfected with DT960 construct. Foci were detected by FISH and manually counted on a fluorescent microscope.

The percentage of HeLa cells (figure 3, C) that presented foci was 42% (7% with one focus, 8% with two foci, 7% with two to four foci and 20% presented more than four foci). This numbers suggest that at least 42% of HeLa cells were successfully transfected with the expanded DMPK construct. The actual transfection rate might be higher, as there might be a minor portion of cells, which although successfully transfected with this construct do not form foci.

For T98-G cells (figure 3, B), the transfection result was very similar to HeLa cells. Astrocytes are easier to transfect in compare with neurons. The final result for the population of T98-G is 41% (10% with one focus, 1% with two foci, 15% with two to four foci and 15% presented more than four foci).

SH-SY5Y (figure 3, A) presented the lowest average of foci-positive cells, in comparison with HeLa cells and T98-G, which is not surprising based on the difficulty to transfect neurons on *in vitro* culture. Only 33% had foci (6% with one focus, 7% for two foci, 8% with two to four foci, and 12% present more than 4 foci).

It is possible to confirm that this cell line model system accumulates foci and recreate a molecular hallmark of DM1 making it useful to study the molecular consequences of RNA toxicity.

3. DEREGULACION OF ALTERNATIVE SPLICING IN DM1 CELL MODELS

3.1. RNA extraction and cDNA synthesis:

The RNA of the transfected cell lines with DT960 and DMPKS was extracted. An electrophoresis was performed to check the quality of the extracted RNA. An example is presented in Figure 17 in the appendix, where it is possible to observe a ribosomal RNA population of the expected right size. All the cell lines showed a good quality and not degraded RNA, the gel showed sharp bands, for 28S and 18S.

In order to study the impact of the 960 expanded CTG repeats on the alternative splicing of candidate genes in the three cell lines population (SH- S5Y5, T98-G and HeLa), cDNA was synthesized from RNA. The quality of cDNA was evaluated by semi-quantitative RT-PCR amplification using the β -actin gene. The quality of cDNA was controlled with a positive control of genomic DNA.

In parallel non-transfected (NT), mock, GFP-transfected (Green Fluorescent Protein) and DMPKS samples were used as control. NT was used as control of cell without transfection. Mock transfection is a control that evaluates if the presence of the reagents used in the transfection can cause some effect of alteration of splicing or expression in the cells. GFP was used as a control to evaluate if the presence of a plasmid *per se* can have some defect in the cells. DMPKS was used to evaluate if the defect in the splicing can be caused for the DMPK gene, through the comparison with the effect generated by DT960 plasmids.

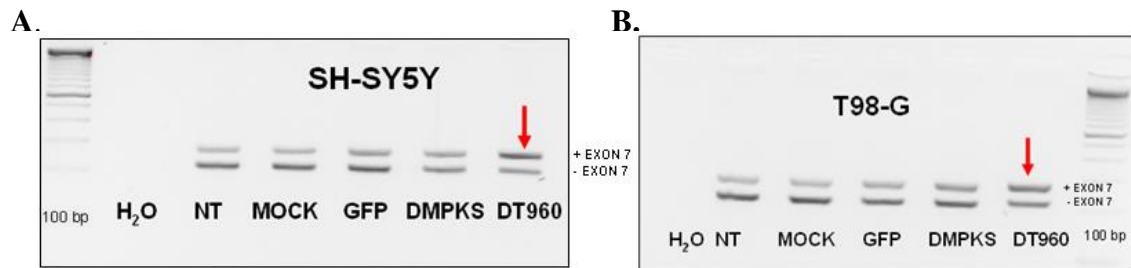
All the sample conditions were homogenized using the β -actin gene expression, testing different quantities of cDNA until all the bands in all the conditions looked with the same intensity of profile. See an example of homogenization cDNA in figure 3 of the Appendix Section.

Once the homogenization was ended, the next step was the analysis of candidate genes to evaluate the alternative splicing. The candidate genes were selected based in two main reasons: previous analysis have shown defects in DM1 patients or mice samples and/or play an important role in calcium metabolism.

3.2. *MBNL1*

In order to test the effect of expanded CTG repeats in the alternative splicing of exon 7 of *MBNL1* and *MBNL2*, a semi-quantitative RT-PCR was performed with oligonucleotides flanking the alternative exon. The analysis was done in SH-SY5Y, T98-G and HeLa cells to assess possible cell type-specific effects. Non-transfected, mock-transfected and DMPKS-transfected controls were included in the analysis, as previously described.

Figure 4 shows an example of the analysis of the *MBNL1* gene in the three cell lines, for all the conditions tested. The amplification generated two products with the following sizes: 216bp, corresponding to the isoform containing exon 7, and 162bp corresponding to the isoform non-containing exon 7.



Quality One Software 4.6.3.

Figure 4. *MBNL1* PCR to evaluate the missplicing in the exon 7. The graphs represent the splicing defect in SH-SY5Y (A) and T98-G (B) cells; NT: cell with non-transfection; Mock: cells with mock-transfection, GFP: cells transfected with the GFP plasmid; DMPKS: cells transfected with short CTG repeats insert (DMPKS); DT960: cells transfected with expanded CTG repeats (DT960); H₂O: used to evaluate the non-contamination in the PCR; 100bp: 100bp molecular weight ladder; red arrow: remark the change of profile from all the conditions in comparison with DT960 sample; + exon 7: isoform containing exon 7; -exon 7: isoform non-containing exon 7.

The analysis revealed that the intensity of the band corresponding to the inclusion of exon 7 increases in DT960-transfected cells, compared to all the other controls. This result appears to be true for SH-SY5Y and T98-G cells, indicating that the expression of toxic CTG repeats in this cell lines affect the alternative splicing of this gene, inducing an abnormal inclusion of exon 7.

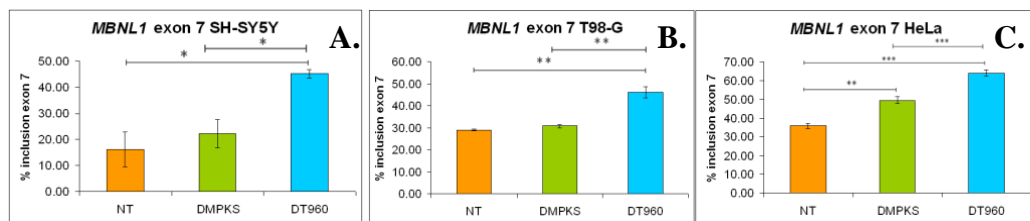
The results show that mock and GFP transfection do not greatly affect alternative splicing. However, the overexpression of DMPK without repeats (DMPKS plasmid) may already have an effect on the splicing of target genes, which is accentuated by the presence of the CTG repeats.

In order to quantify the inclusion of exon 7 in *MBNL1*, three samples with transfected cell lines have been repeated to analysis the alternative splicing, using three independent replicates for each condition tested: non-transfected, DMPKS- and DT960-transfected. Since mock and GFP transfection do not alter the splicing pattern, when compared to non-transfected cells, these controls had been excluded from the quantitative analysis (see figure 4).

The intensity of the bands was determined with the Quality One Software 4.6.3. and the ratio of inclusion of the alternative exon for each independent replicate has been calculated with the Microsoft Excel Software as follows: **(intensity of “+exon 7” band)/[(intensity of “+exon 7” band)+(intensity of “-exon 7” band)] x100.**

Results are shown in figure 5. Statistically significant differences were assessed by student t-test. Representative gels used for the quantification are shown in the Appendix Section (see appendix number 7).

There is an increasing of the inclusion of the exon 7 in different cell lines SH-SY5Y (figure 5, A), T98-G (figure 5, B) and HeLa (figure 5, C) transfected with DT960. The relations DT960/DMPKS and DT960/ NT did not show significant statistical results for SH-SY5Y and T98-G. Also it is important to remark the existence of a significant difference between NT/DMPKS for HeLa cell lines checking what was regarded in the qualitative data. DMPK gene could generate a missplicing effect in some genes; this is seen increasingly in the presence of the expansion of the CTG repeats.



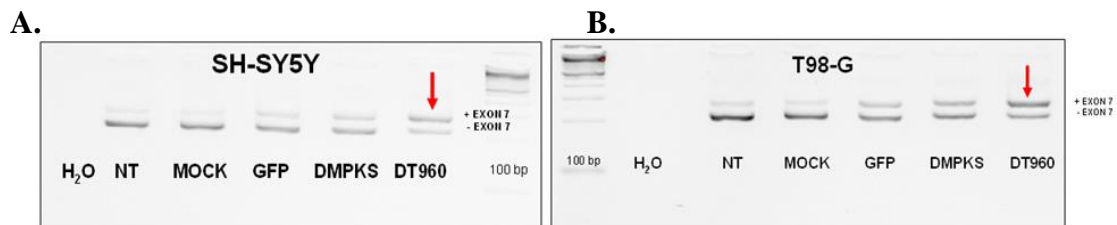
Microsoft Excel Software

Figure 5. Quantitative analyses of *MBNL1* exon 7 missplicing. The picture represent the average ratio of inclusion of exon 7 (\pm SD) in SH-SY5Y (A), T98-G (B) and HeLa cells (C) under three different conditions: non-transfection (NT), transfection with control short DMPK construct (DMPKS); transfection with expanded DMPK construct (DT960) statistically significant differences were assessed by student t-test (*, $p < 0,05$; **, $p < 0,01$ and ***, $p < 0,001$).

In synthesis, the quantitative analyses of *MBNL1* splicing defects in SH-SY5Y, T98-G and HeLa cells showed the expression of expanded CTG repeats affects exon 7 splicing and increases its inclusion ratio. This is primary good evidence that these cell lines recreate important aspects of RNA toxicity associated with DM1, notably abnormal alternative splicing of target genes known to be affected in DM1 patients and mouse models of the disease.

3.3 *MBNL2*:

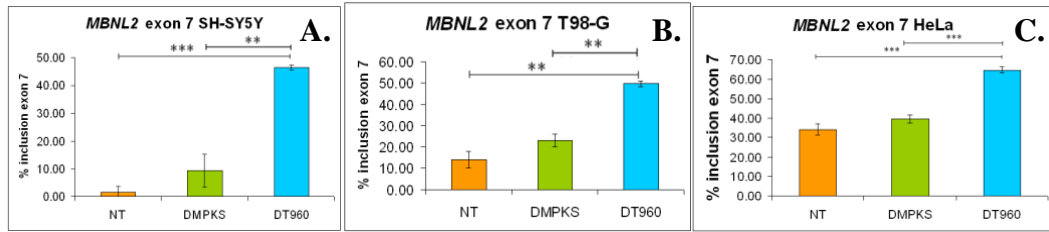
The quantitative analysis of *MBNL2* for alternative splicing was performed as for *MBNL1*, and they revealed the amplification of two products with the following sizes: 212bp, corresponding to the inclusion of exon 7, and 158bp corresponding to the exclusion of exon 7 (figure 6).



Quality One Software 4.6.3.

Figure 6. *MBNL2* PCR to evaluate the missplicing in the exon 7. The picture represent the splicing defect in SH-SY5Y (A) and T98-G (B) cells; NT: cell with non-transfection; Mock: cells with mock-transfection, GFP: cells transfected with the GFP plasmid; DMPKS: cells transfected with short CTG repeats insert (DMPKS); DT960: cells transfected with expanded CTG repeats (DT960); H₂O: used to evaluate the non-contamination in the PCR; 100bp: 100bp molecular weight ladder; red arrow: remark the change of profile from all the conditions in comparison with DT960 sample; + exon 7: isoform containing exon 7; -exon 7: isoform non-containing exon 7.

The identical analysis of *MBNL2* generated similar results; they indicated an increase of inclusion of exon 7 in cells expressing CTG expansions repeats (figures 20, 21, 22 from the appendix). A mild effect could also be observed when the cells were transfected with no-repeat DMPKS construct. Otherwise this minor effect is not significant in compared to NT (see figure 7).



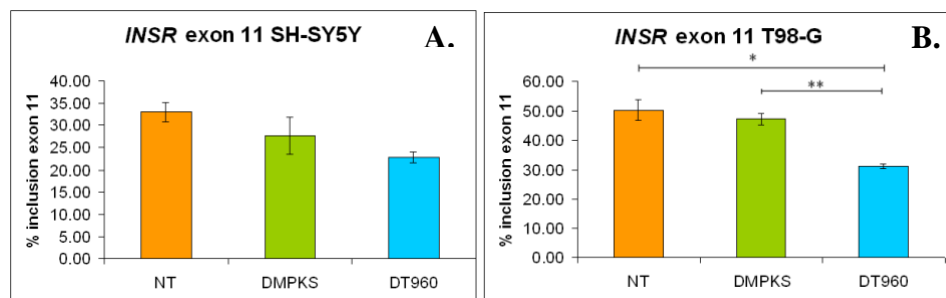
Microsoft Excel Software

Figure 7. Quantitative analyses of *MBNL2* exon 7 missplicing. The graphs represent the average ratio of inclusion of exon 7 (\pm SD) in SH-SY5Y (A), T98-G (B) and HeLa cells (C) under three different conditions: non-transfection (NT), transfection with control short DMPK construct (DMPKS); transfection with expanded DMPK construct (DT960) statistically significant differences were assessed by student t-test (*, $p < 0,05$; **, $p < 0,01$ and ***, $p < 0,001$).

It is important to mention the inclusion of the exon 7 in all the cell lines (SH-SY5Y, T98-G and HeLa cells) for *MBNL2* under the DT960-transfection condition.

3.4 *INSR*:

The semi-quantitative RT-PCR analysis of SH-SY5Y (A) and T98-G (B) generated two products with the following sizes: 165bp, corresponding to the exclusion of exon 11, and 129bp corresponding to the inclusion of exon 11 of *INSR* (the figure 20 and 21 in the appendix illustrated the results). HeLa cells did not show the expression of the two alternative splicing isoform for *INSR* (figure 22 in the appendix), and showed a lot of unspecific bands on the gel which do the quantification impossible.



Microsoft Excel Software

Figure 8. Quantitative analyses of *INSR* exon 11 missplicing. The graphs represent the average ratio of inclusion of exon 11 (\pm SD) in SH-SY5Y (A) and T98-G (B) cells under three different conditions: non-transfection (NT), transfection with control short DMPK construct (DMPKS); transfection with expanded DMPK construct (DT960) statistically significant differences were assessed by student t-test (*, $p < 0,05$; **, $p < 0,01$ and ***, $p < 0,001$).

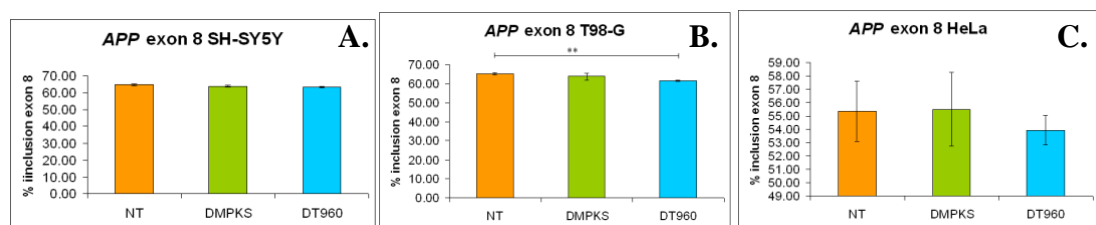
The results (figure 8) show a tendency towards a decreased inclusion of exon 11 in DT960 condition in SH-SY5Y and T98-G cells transfected with large CTG repeat expansions, but the difference in the mean inclusion ratio was not statistically significant when compared to non-transfected and DMPKS control cultures. In contrast, T98-G (figure 8, B) showed significant value for the decreasing of the inclusion of the exon 11 for the condition DMPKS/DT960 and NT/DT960.

The quantitative analysis of *INSR* splicing defects showed a decrease of the exon 11 in *INSR* gene, especially in T98-G cells.

3.5 APP:

The amplification of the *APP* gene was developed to evaluate the splicing defect in SH-SY5Y (A), T98-G (B) and HeLa (C) cells. The semi-quantitative RT-PCR generated two products with the following sizes: 285bp, corresponding to the exclusion of exon 8, and 117bp corresponding to the inclusion of exon 8 isoform of *APP* (figure 9). The two splicing alternative isoforms in the three cell lines was quantified but only T98-G (B) showed a splicing defect between DT960/NT comparisons. See the gels used for the quantification in the figure 20, 21 and 22 in the Appendix Section.

The statistical analysis only revealed significant results in the decrease of the exon 8 in T98-G cells (figure 9, B) for the condition NT/DT960, for the other cell lines (SH-SY5Y and HeLa) there is a mild tendency to the decrease of the inclusion of exon 8 but the average inclusion ratio did not give out statistical significance for the relation NT/DT960 or DMPKS/DT960.



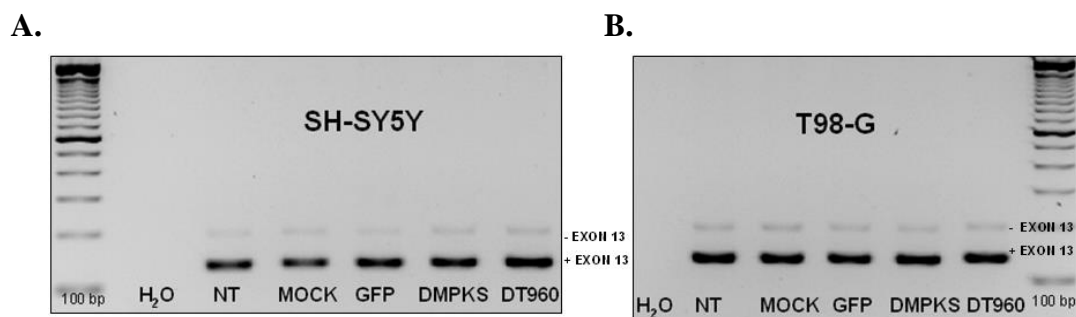
Microsoft Excel Software

Figure 9. Quantitative analyses of *APP* exon 8 missplicing. The graphs represent the average ratio of inclusion of exon 8 (\pm SD) in SH-SY5Y (A), T98-G (B) and HeLa cells (C) under three different conditions: non-transfection (NT), transfection with control short DMPK construct (DMPKS); transfection with expanded DMPK construct (DT960) statistically significant differences were assessed by student t-test (*, $p < 0,05$; **, $p < 0,01$ and ***, $p < 0,001$).

The quantitative analysis of T98-G cells showed missplicing of *APP* gene for the decreasing of exon 8. These results are already confirmed in DM1 patients and transgenic model mouse samples analysed on the laboratory.

3.6. Other genes

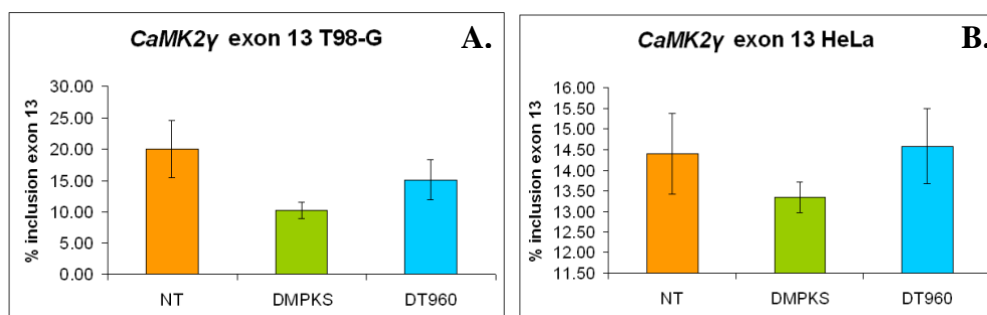
Other genes have been tested, such as *CaMK2 γ* . Two splicing isoforms were detected as 199bp corresponding to the isoform that did non-contain the exon 13 and 136bp associated to the isoform that contained the exon 13. The primary analysis in T98-G and SH-SY5Y showed non-obvious splicing abnormalities of exon 13 in *CaMK2 γ* , for cells with the large expanded CTG repeats (See figure 10).



Quality One Software 4.6.3.

Figure 10. *CaMK2 γ* PCR to evaluate the missplicing in the exon 13. The picture represent the expression of the two isoform corresponding to the alternative splicing in SH-SY5Y (A) and T98-G (B) cells; NT: cell with non-transfection; Mock: cells with mock-transfection, GFP: cells transfected with the GFP plasmid; DMPKS: cells transfected with short CTG repeated insert (DMPKS); DT960: cells transfected with expanded CTG repeats (DT960); H₂O: used to evaluate the non-contamination in the PCR; 100bp: 100bp molecular weight ladder. - exon 13: isoform not-containing exon 13; + exon 13: isoform containing exon 13.

These results were confirmed by semi-quantitative analysis. The intensity of each band was quantified to confirm that this gene did not show a splicing defect for the exon 13 in the gene *CaMK2 γ* in T98-G and HeLa cells (figure 11).



Microsoft Excel Software

Figure 11. Quantitative analyses of *CaMK2γ* exon 13 alternative splicing. The graphs represent the average ratio of inclusion of exon 13 (\pm SD) in T98-G (A) and HeLa (B) cells under three different conditions: non-transfection (NT), transfection with control short DMPK construct (DMPKS); transfection with expanded DMPK construct (DT960).

SH-SY5Y did not present an important visual 136bp band, making the quantification of the alternative splicing not possible for *CaMK2γ* gene (figure 20 in the Appendix Section).

The cells with the expanded CTG repeats do not seem to have an alternative splicing of *CaMK2γ* of exon 13 affected.

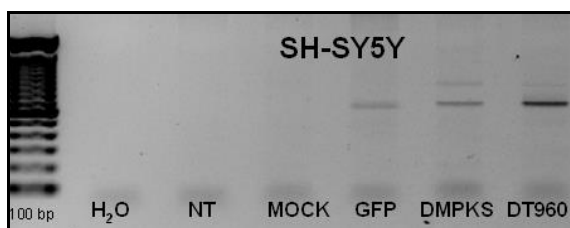
Additional genes such as *NMDAR1* (for exon 5 and exon 21), *CaMK2β* (for exons 18/19/20), *CaMK2δ* (exons 14/15/16), *RyR1* expression, *KCND3* (exon 6) were tested, but semi-quantitative RT-PCR was not sensitive enough to detect their expression in cultured cells. As a result these genes were not subsequently studied. See figure 19 from the appendix to get more details.

4. EXPRESSION DEFECT

4.1 SK3:

Semi-quantitative RT-PCR analyses of candidate genes in the three cell types, under different conditions of transfection provide preliminary evidence about the effect of the CTG repeat expansion on gene expression. Changes in gene expression upon transfection can be measured by variation in the intensity of the bands corresponding to the semi-quantitative RT-PCR amplification products.

The preliminary RT-PCR study suggested increased *SK3* transcript levels in SH-SY5Y cells, in the presence of CTG repeat expansions (figure 12), consistent with the previously reported, upregulation of this gene in DM1 tissue (Kimura *et al.*, 2000).



Quality One Software 4.6.3.

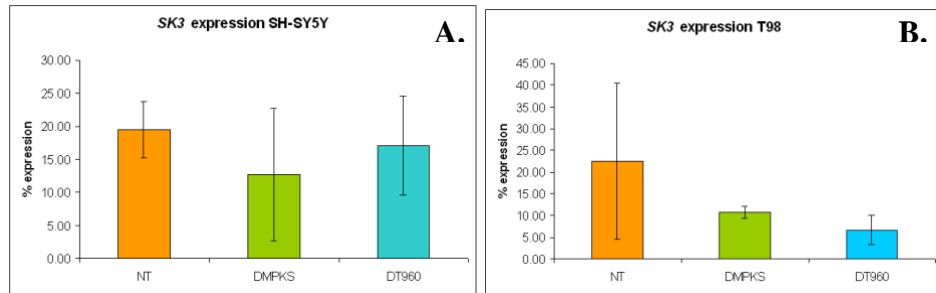
Figure 12. Semi-quantitative RT-PCR analysis of *SK3* transcript in SH-SY5Y cells under different conditions. NT: cell with non-transfection; Mock: cells with mock-transfection, GFP: cells transfected with the GFP plasmid; DMPKS: cells transfected with short CTG repeats insert (DMPKS); DT960: cells transfected with expanded CTG repeats (DT960); H₂O: used to evaluate the non-contamination in the PCR; 100bp: 100bp molecular weight ladder used for checking the right sizes of the bands.

In an attempt to quantify the effect of the CTG repeat expansion on the expression of *SK3* gene, a more detailed semi-quantitative RT-PCR analysis of three samples per transfected cell line was performed.

The intensity of the bands was determined with the Quality One Software 4.6.3. and the level of expression was quantified for each independent replicate and calculated with the Microsoft Excel Software as follows: **(intensity of “gene expression” band)/[(intensity of “ β -ACTIN” band) x100.**

Results are shown in Figure 13, for *SK3* and the means were statistically compared by a t-student statistical test of significance. Representative gels used for the quantification are shown in Figure 20 and 21 in Appendix Section.

Results in figure 13 showed the tendency of the expression decreasing for the *SK3* gene for the cell line SH-SY5Y, but the statistically results did not support this observation with significant values.



Microsoft Excel Software

Figure 13. Semi-Quantitative RT-PCR analyses of the expression of *SK3*. The graphs represent the average of expression (\pm SD) in SH-SY5Y (A) and T98-G (B) cells under three different conditions: non-transfection (NT), transfection with control short DMPK construct (DMPKS); transfection with expanded DMPK construct (DT960).

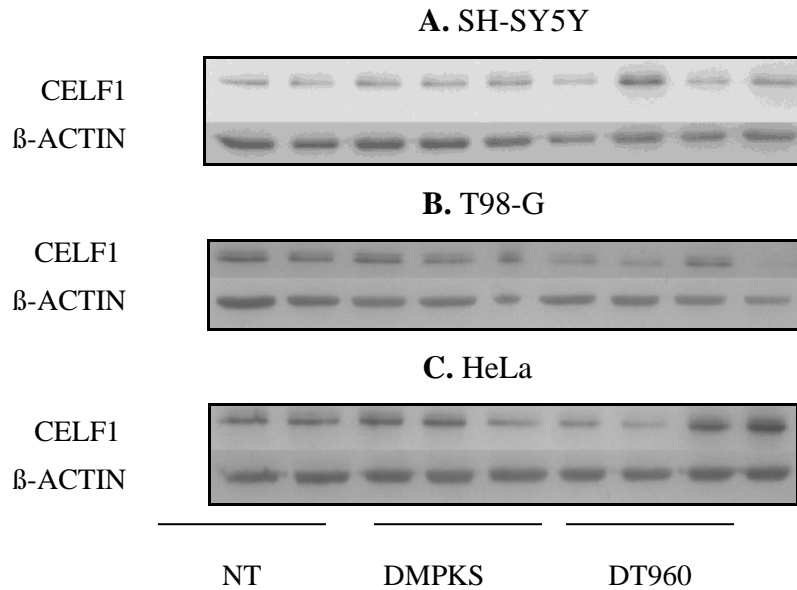
SK3 was also tested in HeLa cells but this cell did not show any expression of this gene. See figure 22 in the Appendix Section.

In contrast to the preliminary results, the analysis has shown that *SK3* gene expression is not altered in DT960-transfected cells (figure 13), when compared to non-transfected of DMPKS controls.

5. PROTEIN EXPRESSION

5.1. CELF1:

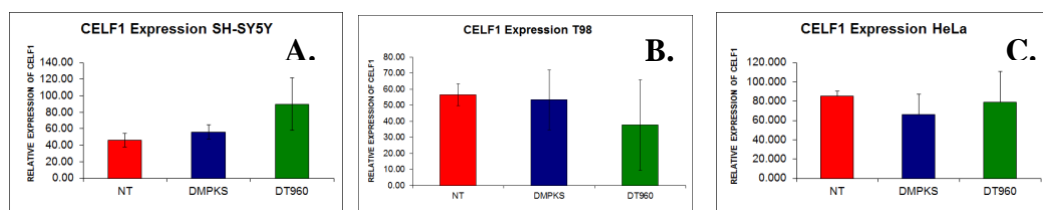
CELF1 upregulation in DM1 muscle and heart contributes to DM1 splicing deregulation (Cooper, 2009). Therefore, it is possible that a similar effect operates in neurons and muscle cells, leading to the splicing defects detected in transfected cells lines. To explore this hypothesis, a quantitative western blot analysis was performed with antibodies directed against CELF1 on protein extracts from non-transfected cells, cells transfected with control DMPKS and transfected with expanded DT960 plasmids (figure 14).



Quality One Software 4.6.3.

Figure 14. Western Blot analyses of CELF1 expression. The picture represent the expression of CELF1 in SH-SY5Y (A), T98-G (B) and HeLa cells (C); NT: cell with non-transfection; DMPKS: cells transfected with short CTG repeats insert (DMPKS); DT960: cells transfected with expanded CTG repeats (DT960); β -actin was used as an internal control to make sure that identical protein quantities were loaded on every lane.

The western blot analysis revealed CELF1 expression in all the cell lines types (SH-SY5Y, T98-G and HeLa) at 50 kDa as size band. The densitometric quantification of bands revealed a tendency of increasing of the expression in SH-SY5Y cells following transfection with large CTG repeat (figure 15); this result is not supported by statistical values.



Microsoft Excel Software.

Figure 15. Quantitative analyses of the CELF1 expression. The graph represents normalized level of CELF1 expression (\pm SD) relative to β -actin in SH-SY5Y (A), T98-G (B) and HeLa cells (C) under three different conditions: non-transfection (NT), transfection with control short DMPK construct (DMPKS); transfection with expanded DMPK construct (DT960).

CELF1 does not show an obvious upregulation in SH-SY5Y, T98-G and HeLa cells upon transfection, suggesting that CELF1 upregulation is not the major mechanism behind missplicing in transfected cells. Nevertheless, the trend detected in neuroblastoma cells, suggests a possibility of CELF1 upregulation in this cell type.

RESULTS DISCUSSION

In order to establish a cell culture model system to study the impact of DM1 mutation on calcium metabolism and homeostasis, the RNA foci accumulation, missplicing and expression of candidate genes and steady-state level of candidate proteins were evaluated in transfected neuroblastoma (SH-SY5Y), astrogloma and (T98-G) and epithelial (HeLa) cells.

The cell lines SH-SY5Y, T98-G and HeLa that had been transfected with CTG expansion construct, presented an important number of foci, recreating an important aspect associated with DM1 pathology. However neither of them presented more than 50% of foci in the total population. It is important to remark the importance of using another technique to insert the CTG expansion repeats in the cells, as infection that can generate 90% of foci in each cell line, as least.

The fact that each cell line presented foci can confirm the presence of toxic RNA accumulation in the nuclei. Other authors have studied fibroblast, myoblast, and muscle and nervous system tissue samples of DM1 patients and have found the accumulation of CUG-containing *DMPK* mutant transcripts (Bermudez & Cisneros, 2008).

The accumulation of toxic RNA in the nuclei generated a splicing defect of MBNL family genes. The results in figure 5 and 7 showed an increase of exon 7 inclusion for *MBNL1* and *MBNL2* in all cell lines. One of the main functions of MBNL proteins is the regulation of the alternative splicing of pre-mRNAs. These proteins have been shown as splicing regulators in skeletal muscle, cardiac tissue and nervous system tissue of MBNL1 and MBNL2 have been shown to colocalize with ribonuclear foci in muscle (in cell culture and tissue) and cortical neurons in DM1 and DM2 (Ranum & Day, 2004).

The splicing defect for *MBNL1* and *MBNL2* exon 7 could give more evidence that the cell line systems reproduce certain aspects of DM1 pathology. Other genes like *INSR* and *APP* showed mild missplicing for T98-G cells (astrocytes). But it is still important to stress that SH-SY5Y cells also presented a tendency of inclusion decreasing for exon 11 of *INSR*. However, the fact that the result was not statistically significant could be explained for the number of nuclear RNA foci in neuroblastoma cells that was just around 30%, perhaps not enough to generate more severe missplicing defect of exon 11 in the overall cell population.

The *MBNL1* missplicing studied in this research depends uniquely on MBNL1 sequestration into nuclear foci, according to previous reports (Kalsotra *et al.*, 2008). These results mean that MBNL1 sequestration (and possibly MBNL2 as well) in the transfected cell lines is sufficient to alter *Mbnl1* exon 7 missplicing.

It would be interesting to detect if CELF upregulation is also responsible for missplicing in these cells. In relation with the study of steady-level of candidate proteins, CELF1 was not upregulated in these cell culture model, however SH-SY5Y showed a pattern of increasing expression level (Figure 16), but a significant difference was not obtained. It is possible that the mean transfection rate, as assessed by the presence of RNA foci (30%) was not enough to detect an obvious effect on CELF1 expression level when looking at the global population of cells. One cannot discard the hypothesis that individual cells could recreate an overexpression of CELF1, but the effect is diluted in the general cell population.

The overexpression of DMPK without repeats (DMPKS plasmid) observed in *MBNL1* for HeLa cells (figure 6), may already have an effect on the splicing of target genes, that is accentuated by the presence of the CTG repeats, maybe through an effect of the DMPK 3'UTR *per se*, in the absence of CTG repeats altering the metabolism of the cell lines. A similar effect was observed through the overexpression of the DMPK 3'-UTR region in wildtype and expanded CTG repeats in DM1 transgenic mice and myoblasts cell culture from DM1 human patients, which delayed muscle development in mice and myoblast differentiation (Sabourin *et al.*, 1997).

APP, *NMDAR1* and *TAU* genes are associated with CNS symptoms, only *APP* presented a mild missplicing defect for T98-G cells lines, SH-SY5Y did not showed splicing defect for *APP*, *NMDAR1* or *TAU*. The need to dedifferentiate the cell could be important to obtain an obvious missplicing of these genes, based on the fact that neuron needs to be differentiating so they can be useful in cell culture.

Some candidate genes as *CaMK2γ* did not show missplicing in SH-SY5Y and T98-G cells, meaning that this gene was not greatly affected for the CTG expanded construct. Other calcium genes *NMDAR1*, *CaMK2β*, *CaMK2δ*, *CACNA2B* and *RyR1* did not express in the cell lines used as model. It is important to extend the research to other calcium candidate genes that could be affected.

SK3 gene did not present an over expression in the SH-SY5Y and T98-G cells which contain the DT960 construct, in contrast with the Kimura *et al.* (2000) previous results, where *SK3* presented upregulation in DM1 skeletal muscle. This could be explained by the fact that *SK3* was evaluated in brain cell lines; perhaps the effect in the brain samples is not as obvious as it is in muscle samples.

In conclusion, brain cells transfected with large CTG repeat expansion within the *DMPK* 3'UTR are a promising model system because they accumulate toxic RNA transcripts and recreate important missplicing events (*MBNL1*, *MBNL2*, *INSR* and *APP*).

Further analysis are required to understand the mechanisms of missplicing, to study the impact of CTG repeat expansions on calcium metabolism and maybe to increase the efficiency of transfection/infection.

CONCLUSIONS

- The presence of foci in SH-SY5Y, T98-G and HeLa cells transfected with long CTG repeats construct validate these cells as a good model system to study the DM1-associated RNA toxicity in brain. Occasionally short CTG repeats construct generates mild splicing defects.
- The missplicing of some candidate genes in SH-SY5Y, T98-G and HeLa cells transfected with long CTG repeats construct recreate some previous results obtained in DM1 human patients and transgenic mice. For example *MBNL1*, *MBNL2* and *INSR* missplicing.
- Candidate calcium genes were not greatly affected by the CTG expanded repeats construct.
- Missplicing in transfected SH-SY5Y, T98-G and HeLa cells is not associated with CELF1 upregulation.

RECOMMENDATIONS

- To confirm if these cell lines are useful as a model system to study the calcium metabolism in brain is essential to use infection as a technique to insert the CTG expanded repeats in the SH-SY5Y, T98-G and HeLa cells, to study additional calcium genes and to use differentiated cells.
- It is necessary to search for the mechanisms involved in splicing deregulation in SH-SY5Y, T98-G and HeLa cells through MBNL1, MBNL2 and MBNL3 co-localization with foci and the steady-state levels of CELF1 and CELF2.
- Measurements of calcium levels and flux should be performed in transfected or infected brain cells to investigate the consequences of the CTG repeat expansion on calcium dynamics and homeostasis.

BIBLIOGRAPHY

- Abe, K. Fujimura, H. Toyooka, K. Yorifuji, S. Nishikawa, Y. Hazama, T. Yanagihara, T. 1994. **Involvement of the central nervous system in myotonic dystrophy.** *Journal of the Neurological Science* (127):179–185.
- Barreau C, Paillard L, Méreau A, Osborne HB. 2006. **Mammalian CELF/Bruno-like RNA-binding proteins: molecular characteristics and biological functions.** **ELSSEVIER Publish.** *Biochimie Journal* 88(5): 515-525.
- Bermúdez, M. Cisneros, B. 2008. **Mini-Review Myotonic Dystrophy 1 in the Nervous System: From the Clinic to Molecular Mechanisms.** *Neuroscience Research Journal* 86: 18–26.
- Botta, A. Vallo, L. Rinaldi, Bonifazi, E. Amati, F. Biancolella, M. Gambardella, S. Mancinello, E. Angelini, C. Meola, G. Novell, G. 2007. **Gene Expression Analysis in Myotonic Dystrophy: Indications for a Common Molecular Pathogenic Pathway in DM1 and DM2.** *Gene Expression Journal* 13: 1-100.
- Brook, D.J. McCurrach, M.E. Harley, H.G. Buckler, A.J. Church, D. Aburatani, H. Hunter, K. Stanton, V.P. Thirion, J.P. Hudson, T. Sohn, R. Zemelman, B. Snell, R.G. Rundle, S.A. Crow, S. Davies, J. Shelbourne, P. Buxton, J. Jones, C. Juvonen, V. Johnson, K. Harper, P.S. Shaw, D.J. Housman, D.E. 1992. **Molecular basis of myotonic dystrophy: Expansion of a trinucleotide (CTG) repeat at the 3' end of a transcript encoding a protein kinase family member.** *Pediatric Neurology Journal* 68: 799-808.
- Cooper, T. 2009. **Neutralizing Toxic RNA.** *Molecular Biology Journal* 32(5938): 272-273.
- Ebralidze, A. Wang, Y. Petkova, V. Ebralidse, K. Junghans, R.P. 2004. **RNA leaching of transcription factors disrupts transcription in myotonic dystrophy.** *Science Journal* 303: 383-387.

- Fardaei, M. Rogers, M.T. Thorpe, H.M. Larkin, K. Hamshere², M.G. Harper, P.S. Brook, J.D. 2002. **Three proteins, MBNL, MBLL and MBXL, co-localize *in vivo* with nuclear foci of expanded-repeat transcripts in DM1 and DM2 cells.** *Human Molecular Genetics Journal* 11(7): 805-814.
- Freshney, I. 2005. **Culture of Animal Cells: A Manual of Basic Technique.** Fifth Edition. PPs : 580
- Gomes-Pereira, M. & Monckton, D.G. 2006. **Chemical modifiers of unstable expanded simple sequence repeats: what goes up, could come down.** *Mutation Research Journal* (598):15-34.
- Gomes-Pereira, M. Foiry, L. Nicole, A. Huguet, A. Junien, C. Munnich, A. Gourdon, G. 2007. **CTG Trinucleotide Repeat “Big Jumps”: Large Expansions, Small Mice.** *Plos Genetic Journal* 3 (4): e52 Pps: 488-491.
- Harper, P.S. Harley, H.G. Reardon, W. Shaw, D.J. 1992. **Anticipation in myotonic dystrophy: new light on an old problem.** *Human Genetic Journal* 51(1): 10-16.
- Harper, P.S. 2001. **Myotonic Dystrophy.** 3rd ed. WB Saunders. Pps: 427.
- Jiang, H. Mankodi, A. Swanson, M. S. Moxley, R.T. Thonrnton, C.A. 2004. **Myotonic dystrophy type 1 is associated with nuclear foci of mutant RNA, sequestration of muscleblind proteins and deregulated alternative splicing in neurons.** *Human Molecular Genetics Journal* 13 (24): 3079-3088.
- Kalsotra, A. Xiao, X. Ward, A. Castle, J.C. Johnson, J.M. Burge, C.B. Cooper, T.A. 2008. **A postnatal swich of CELF and MBNL proteins reprograms alternative splicing in the developing heart.** *Proceeding of the National Academy of the United State of America* 105(51): 20333–20338.

- Kanadia RN, Urbinati CR, Crusselle VJ, Luo D, Lee YJ, Harrison JK, Oh SP, Swanson MS. 2003. **Developmental expression of mouse muscleblind genes Mbnl1, Mbnl2 and Mbnl3.** *Gene Expression Pattern Journal* 3(4): 459-462.
- Kimura, T. Takahashi, M.P. Okuda, Y. Kaido, M. Fujimura, H. Yanagihara, T. Sakoda, S. 2000. **The expression of ion channel mRNAs in skeletal muscles from patients with myotonic muscular dystrophy.** *Neuroscience Letters Journal* 295 (3): 93-96.
- Kohw, Yoshinori. 2004. **Trinucleotide repeat protocols methods in molecular biology.** Edited by Human Press. New Jersey. Volume 277: 334 pps.
- Koshelev M, Sarma S, Price RE, Wehrens XH, Cooper TA. 2010. **Heart-specific overexpression of CUGBP1 reproduces functional and molecular abnormalities of myotonic dystrophy type 1.** *Human Molecular Genetics Journal* 19(6): 1066-1075.
- Linde, C.I. Baryshnikov, S.G Mazzocco-Spezia, A. Golovina, V.A. 2011. **Dysregulation of Ca²⁺ signaling in astrocytes from mice lacking amyloid precursor Protein.** *American Journal of Physiology Cell Physiology* 300(6) 1502-1512
- Liquori, C. Ricker, K. Moseley, M. Jacobsen, J. Kress, W. Naylor, S. Day, J. Ranum, L. 2001. **Myotonic Dystrophy Type 2 Caused by a CCTG Expansion in Intron 1 of ZNF9.** *Journal Science* 293(5531):864-867.
- LGC Standards: www.lgcstandards-atcc.org (June 16th 2011).
- Mankodi, A. Urbinati, C. R. Yuan, Q.P. Moxley, R.T. Sansone, V. Krym, M. Henderson, D. Schalling, M. Swanson, M.S. Thornton, C.A. 2001. **Muscleblind localizes to nuclear foci of aberrant RNA in myotonic dystrophy types 1 and 2.** *Human Molecular Genetics Journal* 10 (19): 2165-2170.

- Meola, G. Sansone, V. Perani, D. Scarone, S. Cappa, S. Dragoni, C. Cattaneo, E. Cotelli, M. Gobbo, C. Fazio, F. 2003. **Executive dysfunction and avoidant personality trait in myotonic dystrophy type 1 (DM-1) and in proximal myotonic myopathy (PROMM/DM-2).** *Journal Neuromuscul Disorder* 13: 813-821.
- Meola, G. Sansone, V. 2007. **Cerebral involvement in myotonic dystrophies.** *Journal Muscle & Nerve* 36: 294–306.
- Michot B, Bachellerie JP, Raynal F. 1983. **Structure of mouse rRNA precursors. Complete sequence and potential folding of the spacer regions between 18S and 28S rRNA.** *Nuclei Acids Research* 11(10): 3375-91.
- Morales, F. Cuenca, P. Brian, R. Sittenfeld, M. Del Valle, G. 2001. **Diagnóstico molecular de la Distrofia Miotónica (DM) en Costa Rica.** *Rev. Acta Médica Costarricense* 43(4): 159-167.
- Modoni, A. Silvestri, G. Pomponi, M.G. Mangiola, F. Tonali, P.A. Marra, C. 2004. **Characterization of the pattern of cognitive impairment in myotonic dystrophy type 1.** *Archives of Neurology* (61):1943–1947.
- Osborne, R.J. and Thornton, C.A. 2006. **RNA-dominant diseases.** *Human Molecular Genetics Journal* 15 (2):162-169.
- Osborne, R.J. Lin, X. Welle, S. Sobczak, K. O'Rourke, J.R. Swanson, M.S. Thornton, C.A. 2009. **Transcriptional and post-transcriptional impact of toxic RNA in myotonic dystrophy.** *Human Molecular Genetics Journal* 18(8):1471-1481.
- Ranum, L. & Cooper, T. 2006. **RNA-Mediated Neuromuscular Disorders.** *The Annual Review of Neuroscience Journal* 29:259–277.
- Ranum, L.& Day, J.D. 2004. **Myotonic Dystrophy: RNA Pathogenesis Comes into Focus.** *The American Society of Human Genetics* 74(5): 793–804.

- Romeo, V. Pegoraro, E. Squarzanti, F. Sorarú, G. Ferrati, C. Ermani, M. Zucchetta, P. Chierichetti, F. Angelini, C. 2010. **Retrospective study on PET-SPECT imaging in a large cohort of myotonic dystrophy type 1 patients.** *Neurological Science Journal* 31(6): 757-763.
- Sabourin, L.A., Tamai, K., Narang, M.A. and Korneluk, R.G. 1997. **Overexpression of 3'-untranslated region of the myotonic dystrophy kinase cDNA inhibits myoblast differentiation in vitro.** *The Journal of Biological Chemistry* 272: 29626–29635.
- Sambrook, J. and Russell, D. 2001. **Preparation of plasmid DNA by Alkaline Lysis with SDS: midiprep.** *Molecular Cloning: A Laboratory Manual*. Third Edition. Volume I. Pps: 1.35-1.37.
- Sergeant, N. Sablonnière, B. Scharaen-Maschke, S. Ghestem, A. Maurage, C.A. Wattez, A. Vermersch, P. Delacourte, A. 2001. **Dysregulation of human brain microtubule-associated tau mRNA maturation in myotonic dystrophy type 1.** *Human Molecular Genetics Journal* 10 (19) : 2143-2155.
- Seznec, H. Agbulut, O. Sergeant, N. Sanvouret, C. Ghestem, A. Tabtl, N. Willer, J.C. Ourth, L. Duros, C. Brisson, E. Fouquet, C. Buther-Browne, G. Delacourte, A. Junien, C. Gourdon, G. 2001. **Mice transgenic for the human myotonic dystrophy region with expanded CTG repeats display muscular and brain abnormalities.** *Human Molecular Genetics Journal* 10 (23): 2717-2726.
- Timchenko LT, Timchenko NA, Caskey CT, Roberts R. 1996. **Novel proteins with binding specificity for DNA CTG repeats and RNA CUG repeats: implications for myotonic dystrophy.** *Human Molecular Genetic Journal* 5(1): 115-121.
- Tsilfidis, C. MacKenzie, A.E. Mettler, G. Barcelo, J. Korneluk, R.G. 1992. **Correlation between CTG trinucleotide repeat length and frequency of severe congenital myotonic dystrophy.** *Nature Genetics* (1): 192–195.

- Wansink, D.G & Wieringa, B. 2003. **Transgenic mouse models for myotonic dystrophy type 1 (DM1).** *Cytogenetic Genome Research Journal* 100: 230-242.
- Ward, A.J. Rimer, M. Killian, J.M. Dowling, J.J. Cooper, T.A. 2010. **CUGBP1 overexpression in mouse skeletal muscle reproduces features of myotonic dystrophy type 1.** *Human Molecular Genetics Journal* 19(18): 3614-3622.
- Winblad, S. Lindberg, C. Hansen, S. 2006. **Cognitive deficits and CTG repeat expansion size in classical myotonic dystrophy type 1 (DM1).** *Behavioral Brain Functions* (2):16.
- Wozniak, J. Mueller, B. Ward, E. Lim, K. Day, J. 2011. **White matter abnormalities and neurocognitive correlates in children and adolescents with myotonic dystrophy type 1: A diffusion tensor imaging study.** *Neuromuscular Disorders* 21: 89-96.
- Zukin R.S, Bennett, M.V. 1995. **Alternatively spliced isoforms of the NMDAR1 receptor subunit.** *Trends in Neuroscience* 18(7):306-313.

APPENDIX SECTION

1. PLASMID STRUCTURES:

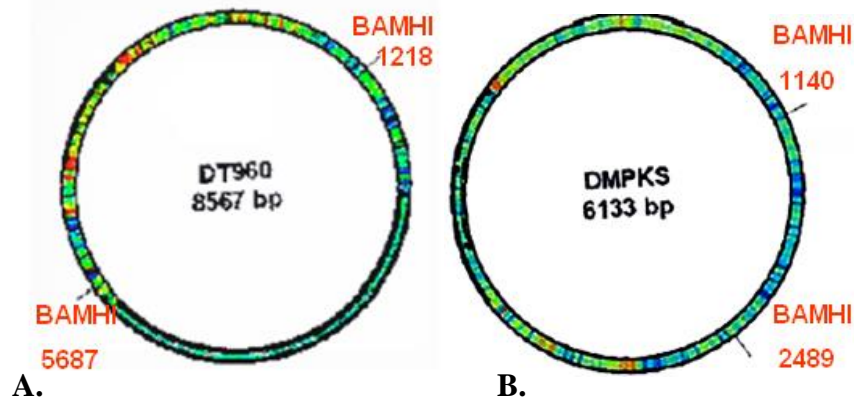


Figure 16. Plasmids used to transfect SH-SY5Y, T98-G and HeLa cell lines. (A) DT960 plasmid (containing expansion of the CTG repeats), the enzyme BAMHI was used to cut the restriction sites (1218 bp and 5687 bp) complete size of the plasmid 8567 bp, (B) DMPKS plasmid (contains short CTG repeats), the enzyme BAMHI was used to cut the restriction sites (1140 bp and 2489 bp), complete size of the plasmid 6133 bp.

2. CELL CULTURE MEDIUM COMPOSITION:

HeLa:

DMEM 1X high glucose (4,5g/L) GLUTAMAX
+ 5% fetal bovine serum (25ml)
+ 100U/ml penicillin streptomycin

Astrocytes T98-G:

DMEM 1X high glucose (4,5 g/L) GLUTAMAX
+ 10% fetal bovine serum (50 ml)
+ 100 U/ml penicillin streptomycin (5ml)
+ 25 µg/ml gentamycin (12,5 ml of 10 mg/ml stock)

Neurons SH-SY5Y:

DMEM (D5648 from SIGMA)
+ 10% foetal bovine serum
+ 100U/ml penicillin and 100 g/ml streptomycin

3. PCR 300 PROTOCOL:

DNA extraction using phenol/chloroform.

Take 15 ng of DNA for a final reaction volume of 25 µl.

Table 1. PCR 300 profile.

Primer oligonucleotide sequences	Reaction conditions	PCR program
Forward primer: 101 5'-CTTCCCAGGCCTGCAGTTTGCCCATC-3'	1X PCR Master Mix (cat: SM-0005 10X+ 4,72 µl β-Mercapto) 0,4 µM reverse primer. 0,4 µM forward primer. 0,04 U Taq DNA polymerase (Integro)	96 °C for 5 min.
Reverse primer: 102 5'-GAACGGGGCTCGAAGGGTCCTTGTAGC - 3'		30 cycles 96 °C for 45s 68 °C for 30s 72 °C for 3 min
		68 °C for 1 min 72 °C for 10 min 10 +∞

Microsoft Office Word Software.

4. OLIGO'S SEQUENCES AND CONDITIONS:

Table 2. PCR's oligonucleotides primers, sequences and conditions.

Evaluated cycles in the quantitative PCR section

GENE	Splicing/Expression	Oligo's 1 name	Oligo 1 sequence	Oligo's 2 name	Oligo 2 sequence	Size	Annealing Temperature (°C)	% Agarose Gel	MgCl ₂	Cycles	SH-SY5Y	T98-G-G	HeLa
HS ¼	Expression (ex8/9)	HS-GS1	AGTCCATGCCATCACTGCCAC	HS-GS2	TCCACCACCCTGTTGCTGTAG	447	59	2	1,5	27	30	30	30
β-ACTINE	Expression (ex8/9)	β-ACTINE-GS1	CCGTCTTCCCCTCCATCG	β-ACTINE-GS2	CCTCGTCGCCACATAGG	87	57	2	1,5	26	21	19	20
MBNL1	Exon 7	hMBNL1-GS1	GCTGCCAATACCAGGTCAAC	hMBNL1-GS2	TGGYGGGAGAAATGCTGTATGC	216/162	57	2,5	1,5	28	25	22/23	24/25/28
MBNL2	Exon 7	hMBNL2-GS1	ACAAGTGACAACACCGTAACCG	hMBNL2-GS2	TTTGGTAAAGGATGAAGAGCACC	212/158	58	3	1,5	29	25	23/24/25	25/29
TAU	Exon 10	hTAU-GS1	GCCACCAGGATTCCAGCAAAAAC	hTAU-GS2	TACGGACCACTGCCACCTTCTTG	244/190	62	2	1,5	30/32/36	-	-	-
NMDAR1	Exon 5	hNMDAR1-GS1	CAGTCCAGCGTGTGGTTGAGATG	hNMDAR1-GS2	TGGCAGAAAGGATGATGACCCG	295/232	60	2,5	1,5	29/36	-	-	29
NMDAR1	Exon 21	hNMDAR1-GS3	CGTGTGGCGGAAGAACCTG	hNMDAR1-GS4	CTGTCTGCGGGGGAGGGG	292/181	60	2,5	1,5	29/36	29	29	29
CaMK2β	Exon 18/19/20	hCaMK2β-GS1	GACAGTGCCAATACCACCATAG	hCaMK2β-GS2	CCTCAAAGTCAACCGTTGTG	481/109	59	2	1,5	29/36	-	-	-
CaMK2γ	Exon 13	hCaMK2γ-GS1	CGTCAGGAGACTGTGGAGAGTGTTGC	hCaMK2γ-GS2	CACCGCCATCCGACTTCTTGTTCC	199/136	61	2,5	1,5	29/36	25	25	29
CaMK2δ	Exon 14/15/16	hCaMK2δ-GS1	TGACAACTATGCTGGCTACAAGG	hCaMK2δ-GS2	TCACATCTTCATCCTCAATTGTTG	117/79	50	3	1,5	28/36	-	-	-
RyR1	Expression	hRyR1-GS1	TTTCTCGCCCCCTGTTTCG	hRyR1-GS2	CTCCTCGTCCCTCCTCCTCTTCTTCC	316	62	2	1,5	32/35	-	-	-
SK3	Expression	hSK3-MGP1	TCATCGCTACCACACACG	hSK3-MGP3	TGCCAGTGAGGAGACAGACAC	585	57	1	1,25	32	27/32	27/32	32
KCND3	Exon 6	hKCND3-GS1	GCAAGACCTCATCATCG	hKCND3-GS2	AGGGACTTCTGTGGATGGTAG	207/150	56	3	1,5	29/34	29	29	29
CACNA2B	Exon 18a	hCACNA2B-GS12	GATGGAAGAAGCAGCCAATC	hCACNA2B-GS13	AGGTTCTGCAGCCGTAGC	231	59	2,5	1,5	31	31	31	31
APP	Exon 8	hAPP-GS1	CCACAGAGAGAACCACCAGCAATGTC	hAPP-GS2	GATACTGTCAACGGCATCAGGGG	285/117	57	2	1,5	30	30	30	30
INSR	Exon 11	hINSR-GS1	CCAAAGACAGACTCTCAGAT	hINSR-GS2	AACATCGCCAAGGGACCTGC	165/129	53	3	1,5	29	29/30	29	29/30
RyR1	Expression	hRyR1-GS3	ATCCTGACTGAAGACCACAGTT	hRyR1-GS4	AGCATAGGCCATGTACAGGTAA	195	55	2	1,5	28	28	28	28

**Information from INSERM U781, took from different articles.*

Microsoft Office Word Software.

5. PROTEIN DETAILS:

Table 3. Gel components concentration.

% of Gel	3,9	4,5	10	12
30% acrylamide/bis (SIGMA A3574)	0,39 ml	2 ml	2,66 ml	3,2 ml
Tris Cl/SDS pH 8,8-1,5 M	0,75 ml (pH 6,8-0,5 M)	2 ml	2 ml	2 ml
Water	1,83 ml	4 ml	3 ml	2,8 ml
APS 10% (SIGMA 7727540)	50 µl	65 µl	65 µl	65 µl
Temed (Invitrogen 15524-010)	5 µl	5,5 µl	5,5 µl	5,5 µl

Microsoft Office Word Software.

Table 4. Buffer Solutions components.

Buffer	Components and preparation of the buffer
5X Electrophoresis Buffer	15,1 g Tris base 94 g Glycine 5 g SDS (25 ml) Water up to 1 L
10X Transfer Buffer	3 g Tris base 14,4 g Glycine 200 ml Methanol 1 g SDS (5 ml) Water up to 1 L
TBS-T 10X	12,1 g Tris base 87,75 g NaCl 5 ml Tween 20 Water up to 1L
Stripping Buffer	1 ml at 20% SDS 78,1 µl β-mercapthoethanol 0,625 ml 1M TrisHCl pH 6,8 Water up to 1L
0,5 M Tris HCl/SDS pH 6,8	6,05 g Tris base in 40 ml of water pH 6,8 (use HCl 1M) Water up 100 ml Filter the solution with 0,45 µl filter 2 ml (0,4 g) SDS
1,5 M Tris-HCl/SDS pH 8,8	91 g Tris base in 300 ml of water pH 8,8 (use HCl 1M) Water up to 500 ml Filter the solution with 0,45 µl filter 10 ml (2 g) SDS
SDS samples buffer 6X	1,5 M Tris-HCl/ SDS pH 8,8 7 ml Glycerol 3 ml SDS 1g (5 ml) Traces of bromophenol blue

Microsoft Office Word Software.

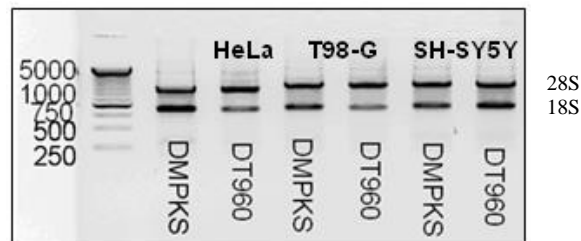
6. ANTIBODIES SOLUTIONS USED BY WESTERN BLOT:

Table 5. Specifications of the Antibodies.

Antibody	Name	Origin	Dilution in 5 ml of 5% Blotho	Dilution in 2 ml of 5% Blotho	MW KDa
β -Actin	-	Mouse	1:3000	-	44
CUGBP1	Anti-CUGBP1	Mouse	1:1000	-	50
IgG-HRP conjugated	Secondary Antibody (anti-mouse)	Sheep	1:7000	-	-

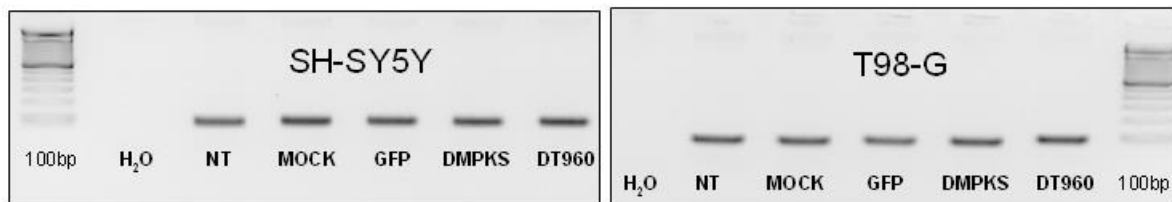
*INSERM U781: "Mechanisms and consequences of CTG repeats instability in a mouse model for myotonic dystrophy"
Microsoft Office Word Software.

7. RNA EXTRACTION AND HOMOGENIZATION:



Quality One Software 4.6.3.

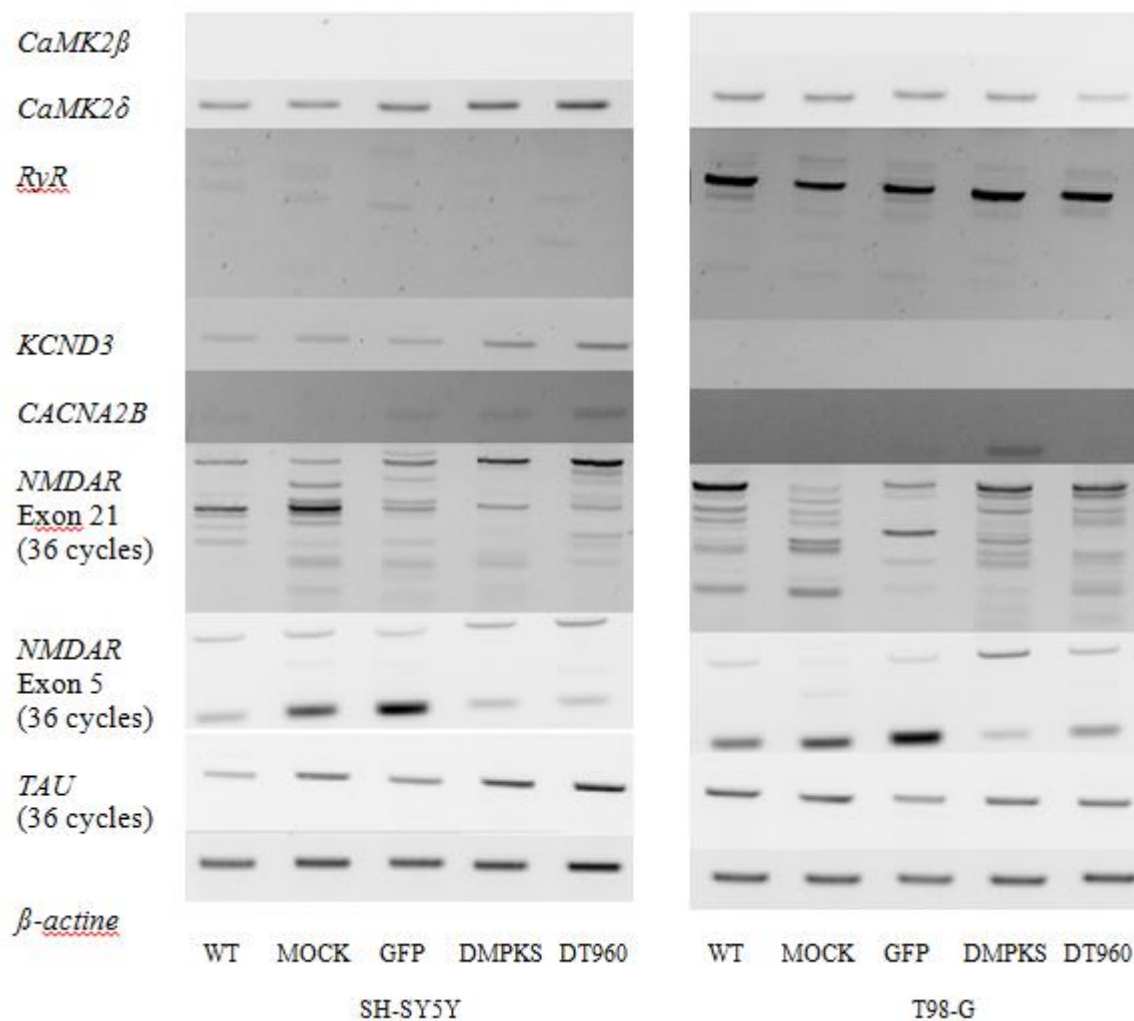
Figure 17. Extracted RNA from SH-SY5Y, T98-G and HeLa transfected cell lines with the plasmids DMPKS and DT960. The ladder in the left shows the different sizes of the bands 18S (999bp) and 28S (1089bp) (Michot *et al*, 1983).



Quality One Software 4.6.3.

Figure 18. Example of β -actin PCR, using in the homogenization of the cDNA samples of transfected T98-G (A) and SH-SY5Y (B) cell lines. NT: cell with non-transfection; Mock: cells with mock-transfection, GFP: cells transfected with the GFP plasmid; DMPKS: cells transfected with short CTG repeats insert (DMPKS); DT960: cells transfected with expanded CTG repeats (DT960); 100 bp: 100bp molecular weight ladder.

8. OLIGOS TESTED GELS PICTURES FROM THE QUALITATIVE RESULTS:

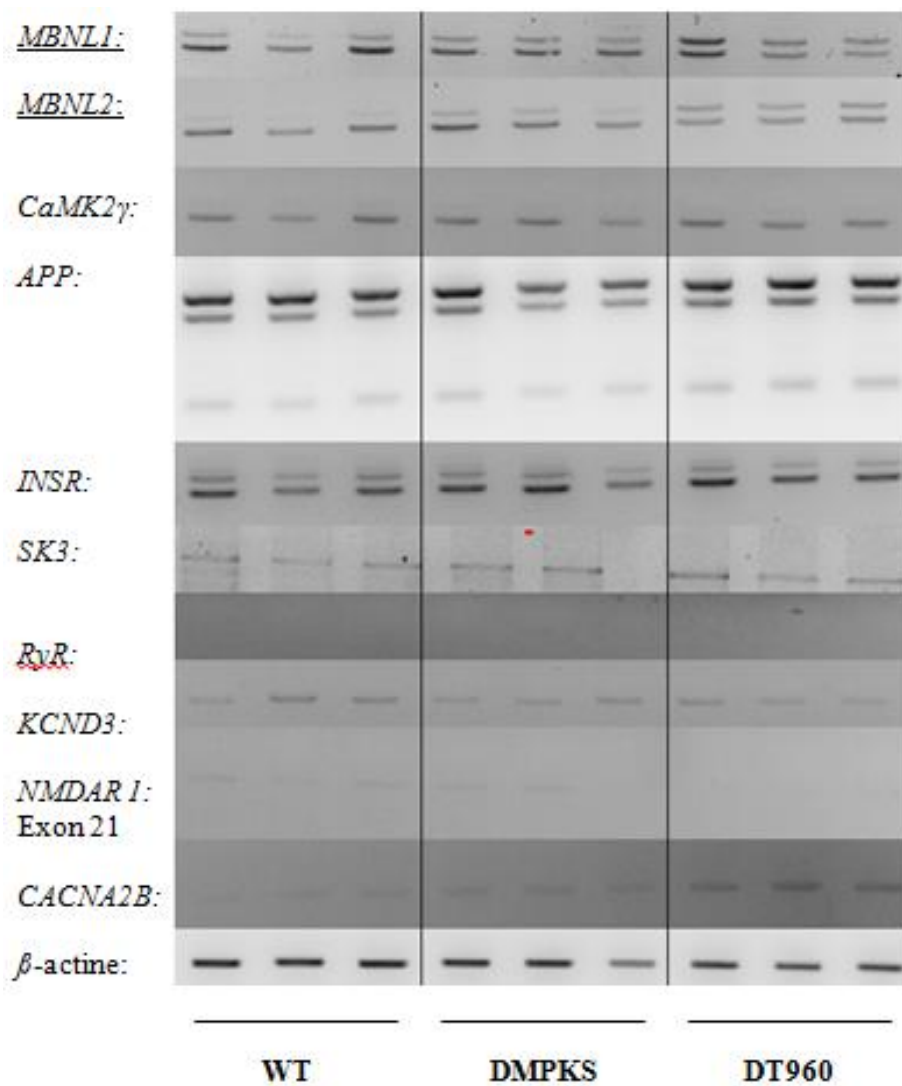


Quality One Software 4.6.3.

Figure 19. Qualitative gels data for check the splicing defect and the expression. These genes did not show expression, splicing defect or right sizes bands. SH-SY5Y (A) and T98-G (B) transfected cell lines under the conditions NT: cell with non-transfection; Mock: cells with mock-transfection, GFP: cells transfected with the GFP plasmid; DMPKS: cells transfected with short CTG repeats insert (DMPKS); DT960: cells transfected with expanded CTG repeats (DT960).

9. OLIGOS TESTED GELS PICTURES FROM THE QUANTITATIVE RESULTS:

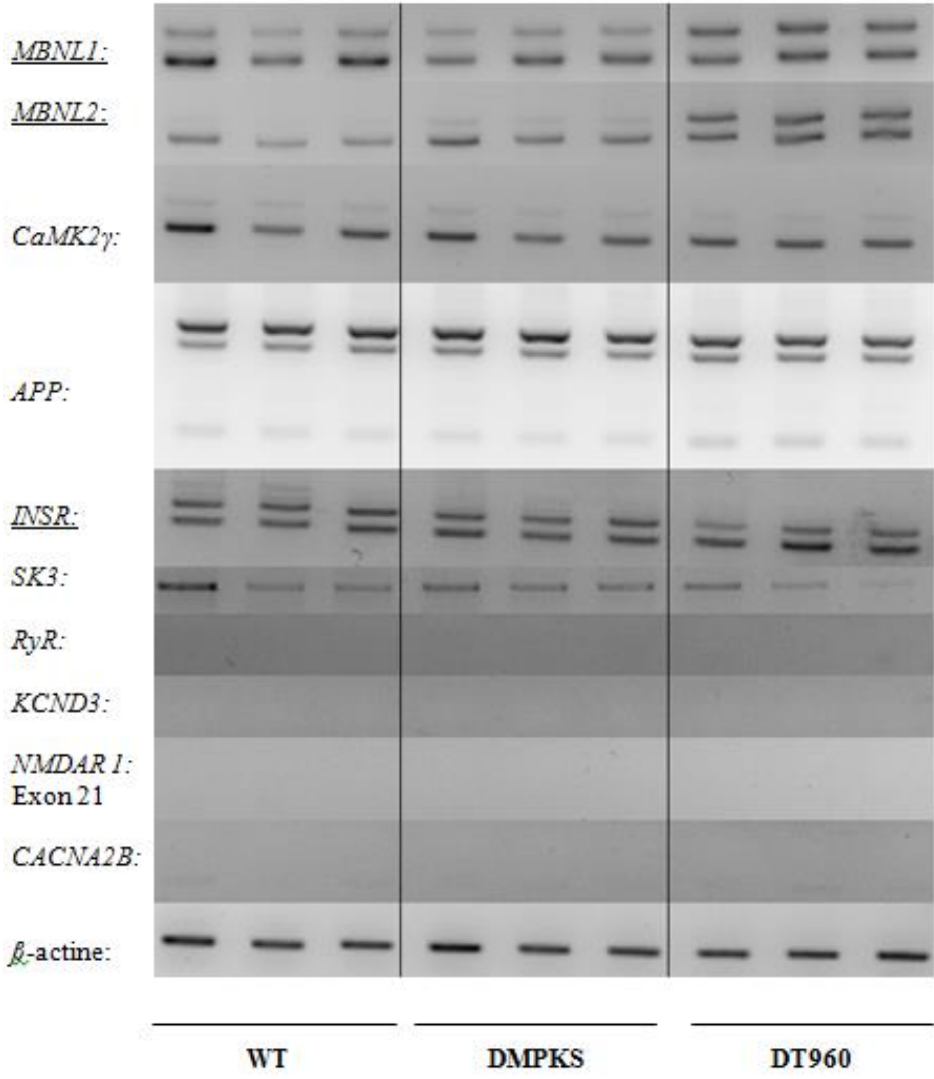
SH-SY5Y cells:



Quality One Software 4.6.3.

Figure 20. Qualitative gels data for check the splicing defect and the expression in transfected SH-SY5Y cells. This gene did not show expression, splicing defect or right sizes bands. Conditions NT: cell with non-transfection; DMPKS: cells transfected with short CTG repeats insert (DMPKS); DT960: cells transfected with expanded CTG repeats (DT960).

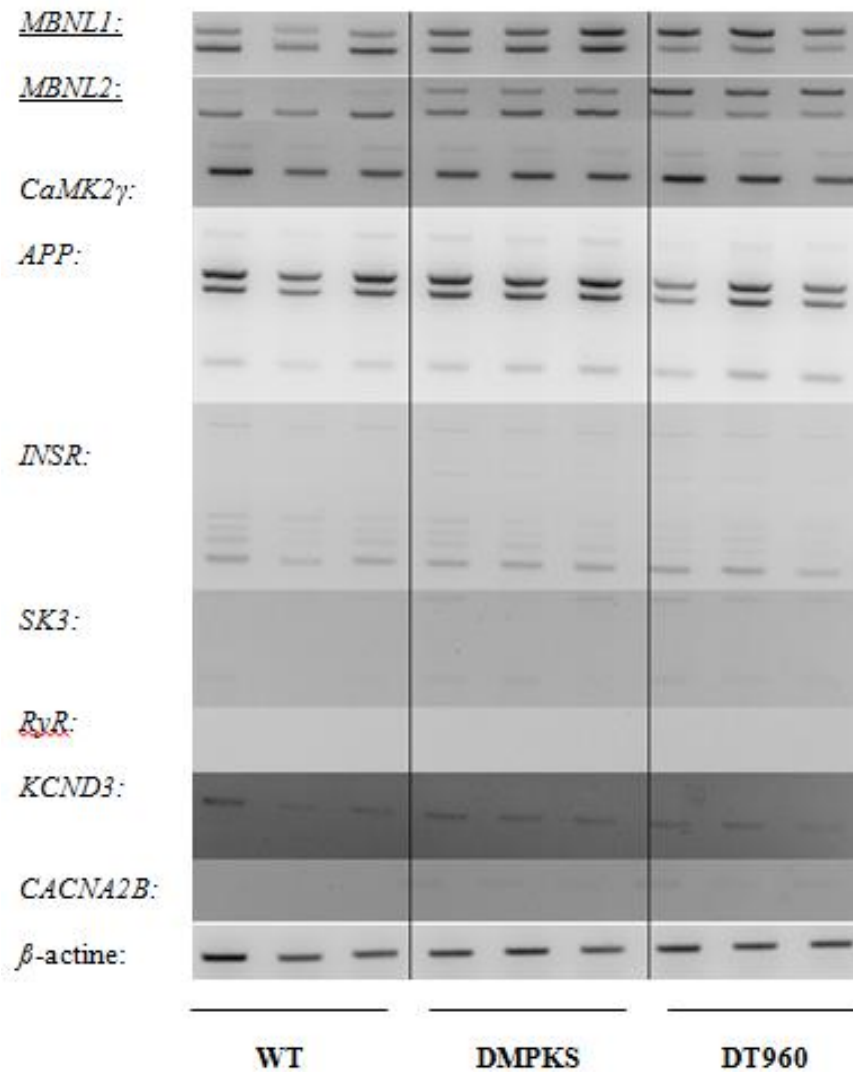
T98-G cells:



Quality One Software 4.6.3.

Figure 21. Qualitative gels data for check the splicing defect and the expression in transfected T98-G cells. These genes did not show expression, splicing defect or right sizes bands. Conditions NT: cell with non-transfection; DMPKS: cells transfected with short CTG repeats insert (DMPKS); DT960: cells transfected with expanded CTG repeats (DT960).

HeLa cells:



Quality One Software 4.6.3.

Figure 22. Qualitative gels data for check the splicing defect and the expression in transfected HeLa cells. These genes did not show expression, splicing defect or right sizes bands. Condition NT: cell with non-transfection; DMPKS: cells transfected with short CTG repeats insert (DMPKS); DT960: cells transfected with expanded CTG repeats (DT960).

10. HOJA DE INFORMACIÓN

Información del estudiante:

Nombre: Annette Diane Vaglio Garro

Cédula: 1-1385-0837

Carné ITCR: 200730732

Dirección de su residencia en época lectiva: Sabanilla, Montes de Oca.

Dirección de su residencia en época no lectiva: Sabanilla, Montes de Oca.

Teléfono en época lectiva: 2280-8055

Teléfono época no lectiva: 2280-8055

Email: ann04vg@gmail.com

Fax: N.A.

Información del Proyecto:

Nombre del Proyecto: Establishment and Characterization of a Brain Cell Culture Model System of Myotonic Dystrophy Type 1.

Profesor Asesor: MSc. Olga Rivas Solano.

Profesor Asesor de la Empresa: PhD. Mario Gomes-Pereira.

Horario de trabajo del estudiante: N.A.

Información de la Empresa:

Nombre: Insitut National de la Santé et de la Rechercher Médicale.

Zona: Paris, Francia.

Dirección: Faculté de Medecine Necker Enfants Malades 149 rue de Sèvres. Tour Lavoisier-2eme étage-75743 Paris cedex 15.

Teléfono: [33] (0)1 40 60 53 34

Fax: [33] (0)1 40 65 54 45

Apartado: 75370 Paris Cedex 15.

Actividad Principal: Investigación de la enfermedad genética DM1.